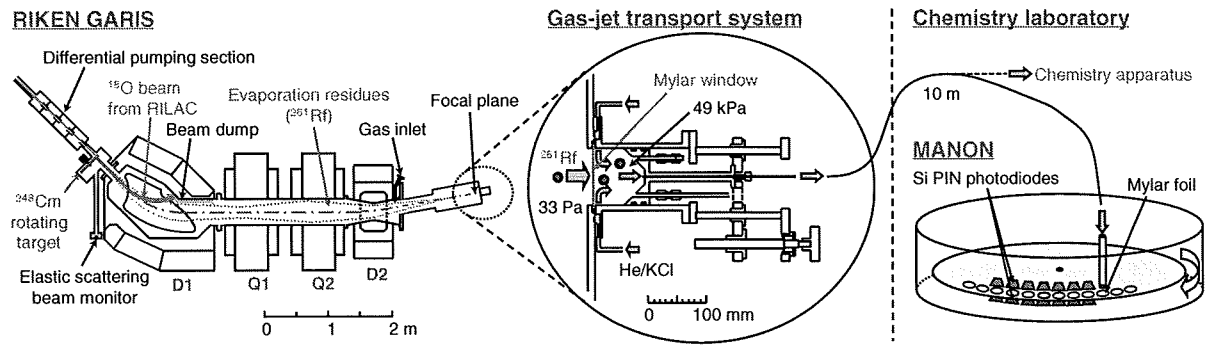

Figure 1. Gas-jet transport system coupled to the RIKEN gas-filled recoil ion separator (GARIS) and the rotating wheel apparatus MANON for α spectrometry placed at the chemistry laboratory.

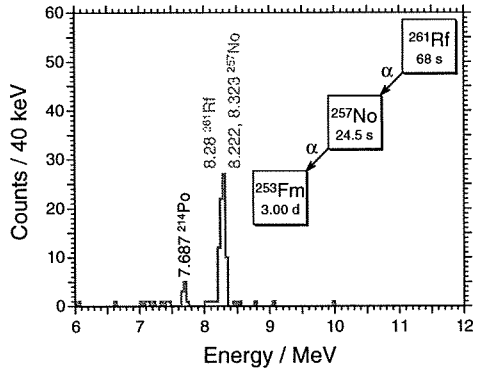

Figure 2. Sum of α-particle spectra measured in the seven top detectors of MANON for 210 s after 30-s aerosol collection.

Figure 2 shows the sum of α-particle spectra measured in the seven top detectors of MANON. The beam dose of 6.3×10^{17} was accumulated. As shown in Figure 2, α peaks of ^{261}Rf (68 s, 8.28 MeV)[11] and its daughter ^{257}No (24.5 s, 8.222 and 8.323 MeV)[11] are clearly seen under the extremely low background conditions. The 7.687-MeV peak is due to ^{214}Po, a descendant of the natural radioisotope ^{222}Rn in the room. The radioactivities due to decays of Po, At, Rn, Fr, Ra, Ac, and Th isotopes, which are largely produced in the transfer reactions on the lead impurity in the target,[12] are fully removed by the present system. A total of 168 α events on ^{261}Rf and ^{257}No were registered in the energy range of interest, including 58 time-correlated α pairs. By comparing the spectrum measured with a focal plane Si detector in a separate experiment, the gas-jet transport efficiency of ^{261}Rf was evaluated to be $52 \pm 12\%$. The transport efficiency of GARIS was $7.8 \pm 1.7\%$ for the focal plane of 100-mm diameter, referring to the cross section of 13 nb.[13]

In this work, we have successfully produced ^{261}Rf for chemical studies in the ^{248}Cm-based hot fusion reaction using the gas-jet transport system coupled to GARIS. The α particles of ^{261}Rf were clearly observed with MANON under the desired low background conditions. The production yield of ^{261}Rf at the chemistry laboratory is 0.5 atoms min^{-1} under the present experimental condition. The present result demonstrates that the GARIS/gas-jet system is promising to explore new frontiers in SHE chemistry: (i) the background radioactivities originating from unwanted reaction products are strongly suppressed, (ii) the intense primary heavy-ion beam is absent in the gas-jet chamber, and hence high gas-jet transport efficiency is achieved, and (iii) the beam-free conditions also make it possible to investigate new chemical systems that were not accessible before.

This experiment was performed at the RI Beam Factory operated by RIKEN Nishina Center and CNS, University of Tokyo. This work was supported by KAKENHI (No. 19002005).

References

1 *The Chemistry of Superheavy Elements*, ed. by M. Schädel, Kluwer Academic, Dordrecht, **2003**.
2 M. Schädel, *Angew. Chem., Int. Ed.* **2006**, *45*, 368.
3 V. G. Pershina, *Chem. Rev.* **1996**, *96*, 1977.
4 P. Schwerdtfeger, M. Seth, in *Encyclopedia of Computational Chemistry*, ed. by P. von R. Schleyer, et al., John Wiley & Sons, Chichester, **1998**, Vol. 4, pp. 2480–2499.
5 R. Eichler, N. V. Aksenov, A. V. Belozerov, G. A. Bozhikov, V. I. Chepigin, S. N. Dmitriev, R. Dressler, H. W. Gäggeler, V. A. Gorshkov, F. Haenssler, M. G. Itkis, A. Laube, V. Y. Lebedev, O. N. Malyshev, Y. T. Oganessian, O. V. Petrushkin, D. Piguet, P. Rasmussen, S. V. Shishkin, A. V. Shutov, A. I. Svirikhin, E. E. Tereshatov, G. K. Vostokin, M. Wegrzecki, A. V. Yeremin, *Nature* **2007**, *447*, 72.
6 C. E. Düllmann, *Eur. Phys. J. D* **2007**, *45*, 75.
7 J. P. Omtvedt, J. Alstad, H. Breivik, J. E. Dyve, K. Eberhardt, C. M. Folden, III, T. Ginter, K. E. Gregorich, E. A. Hult, M. Johansson, U. W. Kirbach, D. M. Lee, M. Mendel, A. Nähler, V. Ninov, L. A. Omtvedt, J. B. Patin, G. Skarnemark, L. Stavsetra, R. Sudowe, N. Wiehl, B. Wierczinski, P. A. Wilk, P. M. Zielinski, J. V. Kratz, N. Trautmann, H. Nitsche, D. C. Hoffman, *J. Nucl. Radiochem. Sci.* **2002**, *3*, 121.
8 J. P. Omtvedt, J. Alstad, T. Bjørnstad, C. E. Düllmann, K. E. Gregorich, D. C. Hoffman, H. Nitsche, K. Opel, D. Polakova, F. Samadani, F. Schulz, G. Skarnemark, L. Stavsetra, R. Sudowe, L. Zheng, *Eur. Phys. J. D* **2007**, *45*, 91.
9 H. Haba, D. Kaji, H. Kikunaga, T. Akiyama, N. Sato, K. Morimoto, A. Yoneda, K. Morita, T. Takabe, A. Shinohara, *J. Nucl. Radiochem. Sci.* **2007**, *8*, 55.
10 H. Haba, H. Kikunaga, D. Kaji, T. Akiyama, K. Morimoto, K. Morita, T. Nanri, K. Ooe, N. Sato, A. Shinohara, D. Suzuki, T. Takabe, I. Yamazaki, A. Yokoyama, A. Yoneda, *J. Nucl. Radiochem. Sci.* **2008**, *9*, 27.
11 C. E. Düllmann, A. Türler, *Phys. Rev. C* **2008**, *77*, 064320.
12 A. Ghiorso, M. Nurmia, K. Eskola, P. Eskola, *Phys. Lett. B* **1970**, *32*, 95.
13 Y. Nagame, M. Asai, H. Haba, S. Goto, K. Tsukada, I. Nishinaka, K. Nishio, S. Ichikawa, A. Toyoshima, K. Akiyama, H. Nakahara, M. Sakama, M. Schädel, J. V. Kratz, H. W. Gäggeler, A. Türler, *J. Nucl. Radiochem. Sci.* **2002**, *3*, 85.

Published on the web (Advance View) March 28, 2009; doi:10.1246/cl.2009.426

^{225}Ac Metallofullerene: Toward ^{225}Ac Nanogenerator in Fullerene

Kazuhiko Akiyama,*[1] Hiromitsu Haba,[2] Keisuke Sueki,[3] Kazuaki Tsukada,[4] Masato Asai,[4]
Atsushi Toyoshima,[4] Yuichiro Nagame,[4] and Motomi Katada[1]
[1]*Graduate School of Science and Engineering, Tokyo Metropolitan University, Hachioji 192-0397*
[2]*Nishina Center for Accelerator-Based Science, RIKEN, Wako 351-0198*
[3]*Graduate School of Pure and Applied Sciences, University of Tsukuba, Tsukuba 305-8577*
[4]*Advanced Science Research Center, Japan Atomic Energy Agency, Tokai, Naka-gun, Ibaraki 319-1195*

(Received August 7, 2009; CL-090737; E-mail: kakiyama@tmu.ac.jp)

We report on the successful production of a metallofullerene encapsulating the radioactive tracer ^{225}Ac and on its electronic properties studied by radiochromatography. Considering the number of π electrons on the fullerene cage estimated from the HPLC retention time on the 5PBB column and the general oxidation state of Ac(III), the chemical species of the dominant chromatographic peak is suggested to be Ac@C_{82}.

Metallofullerenes are extremely interesting and fascinating materials due to their characteristic structures and electronic properties. One of their most attractive characteristics is the ability to encapsulate various species, such as rare earth elements, metal and metal carbide clusters, and noble gas atoms.[1] Recently, fullerenes encapsulating specific radioisotopes have been found to be promising materials for nuclear medical applications. An in vivo experiment with mice using a poly(vinylpyrrolidine) (PVP) emulsion of the radioactive metallofullerenes, ^{140}La@C_{82} and $^{140}La_2$@C_{80}, was conducted by Kobayashi et al.[2] in 1995. The radioactivity of ^{140}La was primarily observed in the liver and blood. Wilson et al.[3] reported the synthesis of metallofullerenols encapsulating ^{166}Ho generated in a nuclear reactor and investigated their biodistribution and metabolism properties. They found that the ^{166}Ho metallofullerenol is localized in the liver. These reports illustrate the possibility using chemically modified metallofullerenes as potential carriers of radioisotopes to targeted organs.

Additionally, α-emitting isotopes with successive cascade decays are anticipated to serve as nanosized radiation generators in the medical and pharmaceutical fields.[4] In 2001, McDevitt et al. reported that the radioisotope ^{225}Ac coupled to internalizing monoclonal antibodies specifically killed leukemia, lymphoma, breast, ovarian, neuroblastoma, and prostate cancer cells at becquerel (Bq) levels.[5] Actinium-225 decays with a half life of 10 d and becomes ^{209}Bi after four α decays and two β decays in succession. An α particle has high linear energy transfer (LET) radiation, and its range in the tissue is about 50 to 80 μm. The exposure of the normal tissue is suppressed low so that ^{225}Ac is considered to be a promising nuclide for radioimmunotherapy. For further application of ^{225}Ac in nuclear medicine, development of more efficient delivery systems is required. As a potential candidate for carriers, a metallofullerene encapsulating ^{225}Ac is one of the most preferable materials. So far, we have successfully produced some metallofullerenes encapsulating lanthanide and actinide elements and studied their electronic properties using radiochromatographic techniques[6–8] which are very sensitive methods and extremely powerful tools for studying the properties of tracer amounts of materials. In this paper, we report the successful production of an ^{225}Ac metallofullerene and on its electronic properties studied by radiochromatography.

The radioactive tracer ^{225}Ac was prepared as an α decay product of ^{229}Th. It was chemically separated by cation exchange from the ^{229}Th and was stored in HNO_3 solution.[9] $La(NO_3)_3$ was added to the solution as a carrier. Next, the solution containing ^{225}Ac and La was adsorbed on a porous carbon rod (10 mmϕ × 60 mm) and was sintered at 800 °C under He atmosphere. The ^{225}Ac metallofullerene was generated by arc discharge using the sintered carbon rod. The products were extracted by CS_2 from the generated soot. The CS_2 solution was filtered to remove the insoluble substance and the filtrate was evaporated to dryness. The dried sample was dissolved in toluene for injection onto a HPLC column of 5PBB (10 mmϕ × 250 mm). The effluent was monitored on-line by a UV absorption detector and was collected on stainless steel disks every 2 min. The HPLC elution behavior of the Ac metallofullerene was determined by α-particle measurements on each fraction. The HPLC chromatogram of the La metallofullerene was also measured by monitoring ^{140}La γ radiation in the eluate with a NaI(Tl) scintillation counter. The radioactive ^{140}La metallofullerene was produced via the thermal neutron irradiation of the separately synthesized crude extract of the La metallofullerene at the JRR3M nuclear reactor at Japan Atomic Energy Agency (JAEA). The sample in toluene was injected onto the 5PBB column under the same developing conditions used for ^{225}Ac.

The production rate of the ^{225}Ac metallofullerene was roughly estimated to be 0.1% from a comparison of the radioactivity in the crude extract of the metallofullerene to that in the solution adsorbed on the porous carbon rod. The rate is almost the same as that for the production of other actinide and lanthanide metallofullerenes.[6,10]

Figure 1 shows the HPLC chromatogram of the ^{225}Ac metallofullerene on the 5PBB column. The chromatogram of the La metallofullerene monitored by NaI(Tl) and that of the hollow fullerenes monitored by UV are also depicted. The elution peak of the Ac metallofullerene is observed at a retention time of 49 ± 1 min which is in good agreement with that of La@C_{82}. It is known that the HPLC retention time on the 5PBB column is well correlated with the number of π electrons on the fullerene cage.[11] Figure 2 shows the logarithm of the retention ratio k of the hollow fullerenes as a function of the number of carbon atoms (the number of π electrons). The retention ratio k is defined as follows:

$$k = (t_R - t_0)/t_0 \quad (1)$$

where t_R is the HPLC retention time of the fullerene, and t_0 is the void retention time (3.79 min) on this column. From a linear

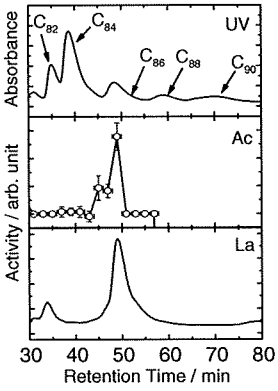

Figure 1. HPLC chromatogram of the Ac metallofullerene on the 5PBB column. The crude extract of the Ac metallofullerene was injected onto the 5PBB column (10 mmϕ × 250 mm) at 6 mL min^{-1}. For comparison, the HPLC chromatogram of the La metallofullerene and that of the hollow fullerenes monitored by UV are also shown.

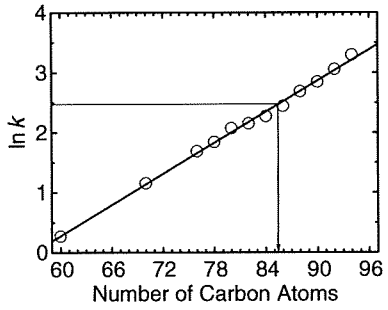

Figure 2. Correlation between the number of carbon atoms and the HPLC retention time of each hollow fullerene: Open circles indicate the retention time of the hollow fullerenes, and the solid line shows the result of the least-squares fit of these open circles. The fitting parameters are as follows: slope = 0.0863 ± 0.0014 and section = 4.90 ± 0.11.

least-squares fit, the number of π electrons on the fullerene cage of the produced Ac metallofullerene is estimated to be 85.5 ± 0.7, which is consistent with the value of La@C_{82} within the error margin.[12] As the most stable oxidation state of Ac is III, it is reasonable to consider that three electrons can transfer from the Ac atom to the fullerene cage. This means that the formal π electrons on the fullerene cage increase by three electrons for each Ac atom.[12] Therefore, Ac@C_{82} (85π electrons) and/or Ac_2@C_{80} (86π electrons) are the possible candidates for the component of the HPLC elution peak. Production of the metallofullerene encapsulating two Ac atoms, however, is negligibly small because the total number of Ac atoms used for the fullerene production is low (10^{10} atoms) and the possibility of the formation of diatomic metallofullerenes of Ac is also extremely low. Thus, Ac@C_{82} is the most potential candidate for the component of the observed elution peak.

In conclusion, the ^{225}Ac metallofullerene was successfully produced. The production rate of the ^{225}Ac metallofullerene was approximately 0.1%. From the HPLC retention time, the Ac@C_{82} species was suggested as the most likely candidate for the metallofullerene.

This work was supported in part by a Grant-in-Aid for JSPS Fellows (17·7096) and by the REIMEI Research Resources of the JAEA.

References

1 a) *Endofullerenes*, ed. by T. Akasaka, S. Nagase, Kluwer Academic, Dordrecht, **2002**. b) T. Braun, H. Rausch, *Chem. Phys. Lett.* **1995**, *237*, 443. c) M. Saunders, R. J. Cross, H. A. Jimenez-Vazquez, R. Shimshi, A. Khong, *Science* **1996**, *271*, 1693. d) S. Stevenson, G. Rice, T. Glass, K. Harich, F. Cromer, M. R. Jordan, J. Craft, E. Hadju, R. Bible, M. M. Olmstead, K. Maltra, A. J. Fisher, A. L. Balch, H. C. Dorn, *Nature* **1999**, *401*, 55.

2 K. Kobayashi, M. Kuwano, K. Sueki, K. Kikuchi, Y. Achiba, H. Nakahara, N. Kananishi, M. Watanabe, K. Tomura, *J. Radioanal. Nucl. Chem.* **1995**, *192*, 81.

3 L. J. Wilson, D. W. Cagle, T. P. Thrash, S. J. Kennel, S. Mirzadeh, J. M. Alford, G. J. Ehrhardt, *Coord. Chem. Rev.* **1999**, *190–192*, 199.

4 a) G. Henriksen, B. W. Schoultz, T. E. Michaelsen, O. S. Bruland, R. H. Larsen, *Nucl. Med. Biol.* **2004**, *31*, 441. b) C. H. Villa, M. R. McDevitt, F. E. Escorcia, D. A. Rey, M. Bergkvist, C. A. Batt, D. A. Scheinberg, *Nano Lett.* **2008**, *8*, 4221.

5 M. R. McDevitt, D. Ma, L. T. Lai, J. Simon, P. Borchardt, R. K. Frank, K. Wu, V. Pellegrini, M. J. Curcio, M. Miederer, N. H. Bander, D. A. Scheinberg, *Science* **2001**, *294*, 1537.

6 K. Akiyama, Y.-L. Zhao, K. Sueki, K. Tsukada, H. Haba, Y. Nagame, T. Kodama, S. Suzuki, T. Ohtsuki, M. Sakaguchi, K. Kikuchi, M. Katada, H. Nakahara, *J. Am. Chem. Soc.* **2001**, *123*, 181.

7 K. Akiyama, K. Sueki, K. Tsukada, T. Yaita, Y. Miyake, H. Haba, M. Asai, T. Kodama, K. Kikuchi, T. Ohtsuki, Y. Nagame, M. Katada, H. Nakahara, *J. Nucl. Radiochem. Sci.* **2002**, *3*, 151.

8 K. Akiyama, K. Sueki, H. Haba, K. Tsukada, M. Asai, T. Yaita, Y. Nagame, K. Kikuchi, M. Katada, H. Nakahara, *J. Radioanal. Nucl. Chem.* **2003**, *255*, 155.

9 K. Akiyama, H. Haba, K. Tsukada, M. Asai, A. Toyoshima, K. Sueki, Y. Nagame, M. Katada, *J. Radioanal. Nucl. Chem.* **2009**, *280*, 329.

10 K. Sueki, K. Kikuchi, K. Akiyama, T. Sawa, T. Katada, S. Ambe, F. Ambe, H. Nakahara, *Chem. Phys. Lett.* **1999**, *300*, 140.

11 a) K. Akiyama, K. Sueki, T. Kodama, K. Kikuchi, Y. Takigawa, H. Nakahara, I. Ikemoto, M. Katada, *Chem. Phys. Lett.* **2000**, *317*, 490. b) S. Okubo, T. Kato, M. Inakuma, H. Shinohara, *New Diamond Front. Carbon Technol.* **2001**, *11*, 285. c) K. Sakaguchi, R. Fujii, T. Kodama, H. Nishikawa, I. Ikemoto, Y. Achiba, K. Kikuchi, *Chem. Lett.* **2007**, *36*, 832.

12 For recent reviews, see: a) D. S. Bethune, R. D. Johnson, J. R. Salem, M. S. de Vries, C. S. Yannoni, *Nature* **1993**, *366*, 123. b) S. Nagase, K. Kobayashi, T. Akasaka, *Bull. Chem. Soc. Jpn.* **1996**, *69*, 2131. c) S. Nagase, K. Kobayashi, T. Akasaka, T. Wakahara, in *Fullerenes: Chemistry, Physics and Technology*, ed. by K. Kadish, R. S. Ruoff, John Wiley & Sons, New York, **2000**, pp. 395–436.

Published on the web (Advance View) September 12, 2009; doi:10.1246/cl.2009.978

Chloride Complexation of Zr and Hf in HCl Investigated by Extended X-ray Absorption Fine Structure Spectroscopy: Toward Characterization of Chloride Complexation of Element 104, Rutherfordium (Rf)

Hiromitsu Haba,*[1] Kazuhiko Akiyama,[2] Kazuaki Tsukada,[3] Masato Asai,[3] Atsushi Toyoshima,[3] Tsuyoshi Yaita,[3] Masaru Hirata,[3] Keisuke Sueki,[4] and Yuichiro Nagame[3]

[1]Nishina Center for Accelerator Based Science, RIKEN, Wako 351-0198

[2]Graduate School of Science and Engineering, Tokyo Metropolitan University, Hachioji, Tokyo 192-0397

[3]Advanced Science Research Center, Japan Atomic Energy Agency, Tokai, Naka-gun, Ibaraki 319-1195

[4]Department of Chemistry, University of Tsukuba, Tsukuba 305-8577

Received July 29, 2008; E-mail: haba@riken.jp

Chloride complexation of the group-4 elements Zr and Hf in 8.0–11.9 M HCl is investigated by extended X-ray absorption fine structure (EXAFS) spectroscopy to characterize chloro complexes of the transactinide element, rutherfordium (Rf). The complexes of Zr and Hf successively vary with the concentration of HCl from a hydrated complex $[M(H_2O)_8]^{4+}$ at 8.0 M to a hexachloro complex $[MCl_6]^{2-}$ at 11.9 M (M = Zr and Hf). The present structural changes of the Zr and Hf complexes well reflect the previously studied anion-exchange behavior of Zr and Hf in HCl. From both the EXAFS and anion-exchange results, we suggest that Rf forms the same complexes as those of Zr and Hf in HCl, and that the complexation strength of the hexachloro complexes of the group-4 elements, $[MCl_6]^{2-}$ (M = Zr, Hf, and Rf), is in the sequence of Rf > Zr > Hf.

Chemical characterization of the transactinide elements with atomic numbers $Z \geq 104$ is an extremely interesting and challenging subject in modern nuclear and radiochemistry.[1–5] A most important and interesting question is to clarify chemical properties of these newly-synthesized heavy elements and to elucidate the influence of relativistic effects on chemical properties of these heaviest elements.[1,5–7] The transactinide elements (nuclides) are produced in accelerators in heavy-ion-induced nuclear reactions. Because of the short half-lives and extremely low production rates of these nuclides, chemical experiments with transactinides must be done on an atom-at-a-time scale; spectroscopic studies to characterize chemical species of these elements are not applicable. Experiments with the transactinide elements are usually conducted together with expected lighter homologs in the periodic table using partition methods.[1–5] Observed chemical behavior of the transactinide elements is compared to that of the homologs, and then their properties are discussed based on comparative studies with the homologs.

Pioneering anion-exchange studies of the first transactinide element, rutherfordium (Rf, $Z = 104$), in HCl were performed by Hulet et al.[8] and then Czerwinski et al.[9] The results demonstrated that the chloride complexation of Rf is stronger than that of the trivalent actinide elements and is similar to that of the expected lighter homologs Zr and Hf. In a previous report from our group,[10] the adsorption behavior of Rf together with Zr and Hf on an anion-exchange resin in 4.0–11.5 M HCl was systematically studied using an automated rapid ion-exchange separation apparatus. It was found that the adsorption behavior of Rf is very similar to those of Zr and Hf, suggesting that Rf is a typical member of the group-4 elements. The adsorption strength in the order of Rf > Zr > Hf was also clarified. To deepen our understanding of the anion-exchange behavior and to characterize chemical complexes of Rf, structural data of Zr and Hf complexes in HCl are essentially required. Further, structural information of Rf inferred from comparative studies with Zr and Hf is also available to perform theoretical molecular orbital calculations and to discuss the electronic structure of Rf.

The extended X-ray absorption fine structure (EXAFS) measurements can provide information on the local environment around the central atom such as the atomic number (Z), the number of neighboring atoms (N), and their distance from the central atom (R). In the present work, we have measured the EXAFS spectra of Zr and Hf complexes in 8.0–11.9 M HCl and those of Zr complexes on an anion-exchange resin equilibrated with 9.0–11.9 M HCl. The structural changes of these complexes with the HCl concentration are discussed by referring to our anion-exchange results for Zr and Hf.[10] Based on both the EXAFS and anion-exchange results for the chloride complexation of Zr and Hf, we discuss the formation of chloro complexes of Rf in HCl.

Experimental

Commercially available $ZrCl_4$ and $HfCl_4$ powders were dissolved with 8.0, 9.0, 9.5, 10.0, 10.5, 11.0, 11.5, and 11.9 M HCl to obtain 0.01 M concentration of Zr and Hf. The concentrations of the HCl solutions were determined by titration with a standardized

Published on the web June 12, 2009; doi:10.1246/bcsj.82.698

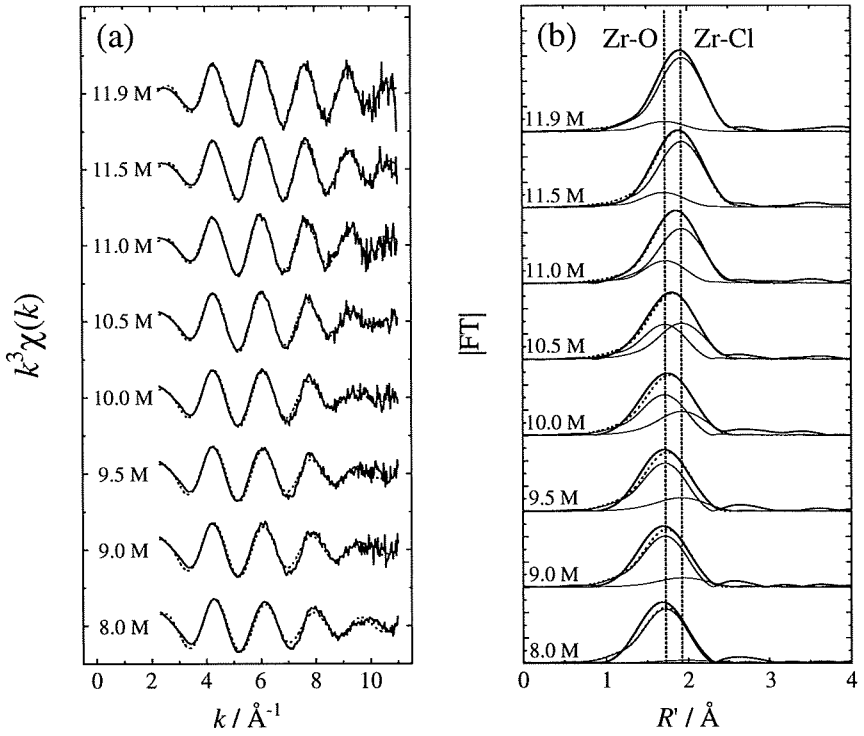

Figure 1. (a) The k^3-weighted raw EXAFS spectra of the Zr complexes in 8.0, 9.0, 9.5, 10.0, 10.5, 11.0, 11.5, and 11.9 M HCl (thick solid curves) and (b) the corresponding radial structural functions (thick solid curves). The theoretical fits by FEFF 7 (Ref. 12) are shown by dotted curves. The radial structural functions are decomposed into two components for the shells M–O and M–Cl (thin solid curves). The peak positions for the Zr–O and Zr–Cl shells are indicated by vertical dashed lines.

NaOH solution. Five hundred μL of each sample solution was pipetted and sealed in a polyethylene bag. For the resin samples, the anion-exchange resin used was MCI GEL CA08Y, supplied by Mitsubishi Chemical Corporation in a chloride form, a strongly basic quaternary-amine polymer with a particle size of 22 ± 2 μm. 100 mg of CA08Y and 5 mL of the 0.002 M Zr solutions in 9.0, 10.0, and 11.9 M HCl were added into a polypropylene tube and were equilibrated for 30 min. The mixture was sealed in the polyethylene bag. It is noted that the distribution coefficient (K_d) of Zr on CA08Y is more than 140 mL g^{-1} at ≥9.0 M where most of Zr–chloro complexes are adsorbed on the resin.[10]

EXAFS spectra were collected at BL27B of the High Energy Accelerator Research Organization Photon Factory (KEK-PF) using a Si(111) monochromator. Measurements were performed in the fluorescence mode at the Zr K edge and the Hf L_{III} edge with a 7-element Ge detector. Twenty-five to 40 scans were collected for each sample to obtain statistically significant data.

The EXAFS spectra were analyzed according to standard procedures using the WinXAS 3.1 code.[11] The radial structural functions were obtained by Fourier transformation of the EXAFS oscillations in the k space in the range of 2.3–11.0 Å^{-1} for Zr and 1.5–11.0 Å^{-1} for Hf. Fitting analyses were conducted using the backscattering amplitude and phase shift parameters calculated by the ab initio curved-wave multiple-scattering program FEFF 7.[12] Free parameters were the Debye–Waller factor (σ^2), the distance to the neighboring atom (R), the number of neighboring atoms (N), and the relative energy threshold (ΔE_0). The fixed reduction factor (S_0^2) was included in the present analysis to make it possible to systematically compare the complex structures of Zr and Hf as a function of the HCl concentration. The reduction factor of $S_0^2 = 1.10$ was determined by assuming the octahedral hexachloro complex of Zr, $[ZrCl_6]^{2-}$, in 11.9 M HCl as suggested by Raman spectroscopic studies;[13,14] N was fixed to 6, and S_0^2, σ^2, R, and ΔE_0 were free. Errors estimated from the fits to well-characterized model compounds are ±20% for N and ±0.02 Å for R.

Results and Discussion

The k^3-weighted raw EXAFS spectra of the Zr complexes in 8.0, 9.0, 9.5, 10.0, 10.5, 11.0, 11.5, and 11.9 M HCl are shown in Figure 1a together with the theoretical fits by FEFF 7 indicated by dotted curves. The corresponding radial structural functions are depicted in Figure 1b. Note that the R' shown in Figure 1b is not corrected for the EXAFS phase shifts. The analytical results for Hf are given in Figure 2. The fitting parameters, N, R, σ^2, and ΔE_0 for Zr and Hf complexes are summarized in Tables 1 and 2, respectively.

The structural changes of the Zr and Hf complexes are very similar to each other in the HCl concentration range studied. In Figures 1b and 2b, the radial structural functions (thick solid curves) are successfully decomposed into two components corresponding to the shells of M–O and M–Cl (M = Zr and Hf) as shown by thin solid curves. The peak positions for these shells are indicated by vertical dashed lines. At 8.0 M, the M–O peak from the M–OH_2 and/or M–OH bonds is dominant for both Zr and Hf. The R values were determined to be 2.23 and 2.20 Å for the Zr–O and Hf–O shells, respectively, and the N values are 7.4 and 8.0. It is known that the M–OH_2 and M–OH distances in the various oxygen-containing compounds in eight-coordination are in the ranges 2.20–2.29 and 2.10–2.14 Å, respectively.[15] Thus, the water-containing complex structure of

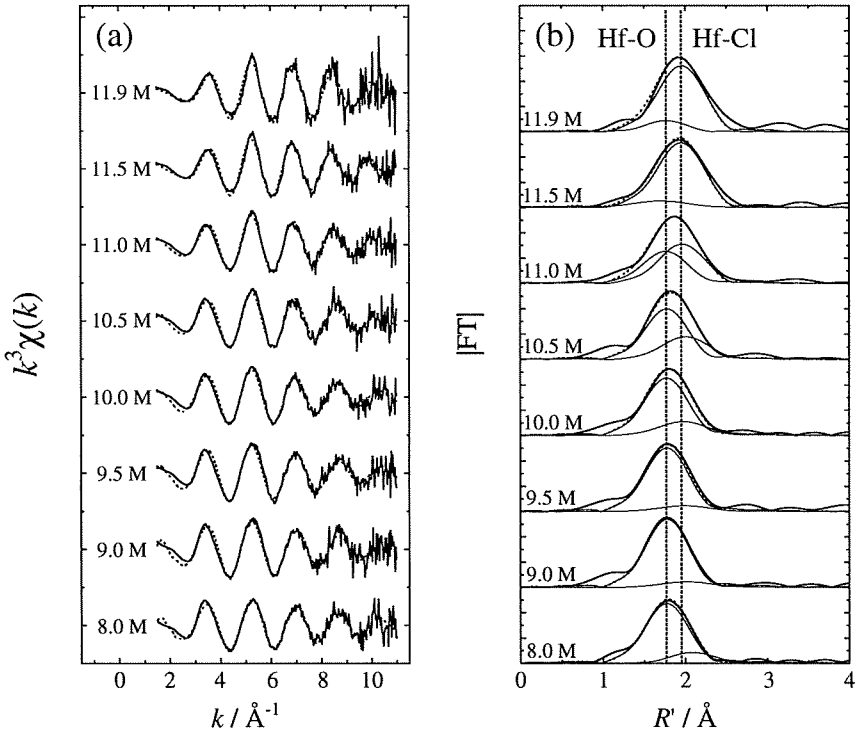

Figure 2. (a) The k^3-weighted raw EXAFS spectra of the Hf complexes in 8.0, 9.0, 9.5, 10.0, 10.5, 11.0, 11.5, and 11.9 M HCl and (b) the corresponding radial structural functions. See the caption of Figure 1 for other details.

Table 1. EXAFS Structural Parameters of the Zr Complexes in 8.0–11.9 M HCl

[HCl] /M	Zr–O				Zr–Cl			
	N	R /Å	σ^2	ΔE_0 /eV	N	R /Å	σ^2	ΔE_0 /eV
8.0	7.4	2.23	0.0082	2.90	0.7	2.56	0.0209	9.80
9.0	7.5	2.23	0.0088	0.61	1.4	2.48	0.0161	4.51
9.5	6.7	2.23	0.0083	0.37	2.3	2.48	0.0165	2.51
10.0	6.1	2.24	0.0088	−0.20	3.0	2.47	0.0126	1.92
10.5	4.2	2.23	0.0065	−0.30	3.7	2.46	0.0098	0.46
11.0	2.0	2.23	0.0030	−1.36	5.0	2.46	0.0084	−1.01
11.5	1.3	2.22	0.0032	−5.22	6.1	2.46	0.0086	−0.54
11.9	0.6	2.21	0.0008	−5.15	6.3	2.46	0.0075	−0.81

Table 2. EXAFS Structural Parameters of the Hf Complexes in 8.0–11.9 M HCl

[HCl] /M	Hf–O				Hf–Cl			
	N	R /Å	σ^2	ΔE_0 /eV	N	R /Å	σ^2	ΔE_0 /eV
8.0	8.0	2.20	0.0090	5.21	0.7	2.43	0.0063	17.81
9.0	8.6	2.20	0.0083	5.65	0.8	2.40	0.0163	14.77
9.5	8.2	2.20	0.0085	5.17	0.9	2.41	0.0165	9.99
10.0	7.7	2.20	0.0089	4.75	1.7	2.40	0.0132	8.42
10.5	6.1	2.20	0.0075	4.73	2.5	2.42	0.0118	5.91
11.0	4.9	2.20	0.0106	4.43	3.7	2.41	0.0092	3.71
11.5	2.5	2.19	0.0256	3.40	6.8	2.41	0.0103	2.33
11.9	1.0	2.19	0.0038	3.59	6.6	2.41	0.0098	2.97

$[M(H_2O)_8]^{4+}$ is deduced at 8.0 M. Recently, Hagfeldt et al.[16] investigated the complex structures of the hydrated Zr^{4+} and Hf^{4+} ions in concentrated $HClO_4$ by means of EXAFS. Although the Zr–O and Hf–O distances were determined to be 2.187 ± 0.003 and 2.160 ± 0.012 Å, respectively, as in the eight-coordination, these distances are somewhat smaller than the present ones; Hagfeldt et al.[16] pointed out that their experiment cannot rule out the possibility of a seven-coordinated complex with smaller bond distances (≈2.14 Å for Zr–O and ≈2.13 Å for Hf–O). As shown in Figures 1b and 2b, the peak intensity for the M–O shell decreases with an increase of the HCl concentration, while the peaks corresponding to the shell of M–Cl with $R = 2.46$ and 2.41 Å for Zr and Hf, respectively, appear. The N values for M–Cl at 11.9 M are 6.3 and 6.6 for Zr and Hf, respectively, and those for M–O are negligible. The present result confirms the octahedral complex structure of $[MCl_6]^{2-}$ suggested by the Raman spectroscopic studies.[13,14] The present Zr–Cl bond distance agrees well with the literature data of 2.461 ± 0.020 Å averaged for the 24 solid crystals containing $[ZrCl_6]^{2-}$,[17–37] while that for Hf is also consistent with 2.447 ± 0.019 Å for the 14 solid crystals[21,23,27,29,32–35,38–40] within the error limit of the present EXAFS method (±0.02 Å).

In Figure 3, the k^3-weighted raw EXAFS spectra of the Zr complexes adsorbed on the anion-exchange resin CA08Y at 9.0, 10.0, and 11.9 M HCl are shown together with the corresponding radial structural functions. As shown in Figure 3b, only the Zr–Cl peak is observed for the resin samples. The parameters, N, R, σ^2, and ΔE_0, are summarized in Table 3. The average values of $R = 2.48$ Å and $N = 5.9$ agree well with those of the Zr complexes in 11.9 M HCl (see Table 1). The complex structure of Zr and presumably of Hf on the binding site of the anion-exchange resin was found to be $[MCl_6]^{2-}$.

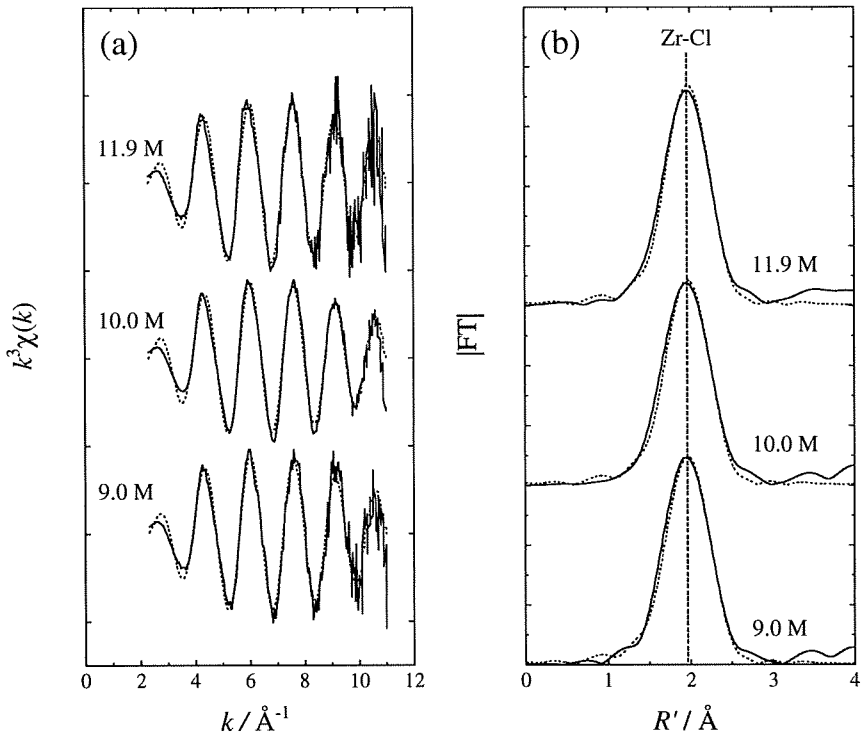

Figure 3. (a) The k^3-weighted raw EXAFS spectra of the Zr complexes adsorbed on the anion-exchange resin CA08Y in 9.0, 10.0, and 11.9 M HCl (solid curves) and (b) the corresponding radial structural functions (solid curves). The theoretical fits by FEFF 7 (Ref. 12) are shown by dotted curves. The peak position for the Zr–Cl shell is indicated by a vertical dashed line.

Table 3. EXAFS Structural Parameters of the Zr Complexes Adsorbed on the Anion-Exchange Resin at 9.0, 10.0, and 11.9 M HCl

[HCl]/M	Zr–Cl			
	N	R/Å	σ^2	ΔE_0/eV
9.0	6.0	2.48	0.0058	0.78
10.0	5.9	2.48	0.0058	0.94
11.9	5.8	2.48	0.0049	1.01

The ratios ρ of the N value for M–Cl ($=N_{Cl}$) to the sum of N for M–Cl and M–O ($=N_{Cl} + N_O$) are shown in Figure 4 as a function of the HCl concentration. The data for Zr and Hf are depicted by closed squares connected with a solid curve and by closed circles with a dotted curve, respectively. The ρ values increase smoothly with an increase of the HCl concentration, reflecting that the chlorinating reaction $[M(H_2O)_8]^{4+} \rightarrow [MCl_6]^{2-}$ successively proceeds. It is noted that the onset HCl concentration, at which the ρ value starts to increase, for Zr is apparently lower than that for Hf. This indicates that the affinity of the Cl^- ion for Zr is stronger than that for Hf.

Previously, we measured the distribution coefficients (K_d) of Zr and Hf on the anion-exchange resin CA08Y in 1.0–11.5 M HCl by a batch method using the radiotracers ^{88}Zr and ^{175}Hf.[10] The K_d values of Zr and Hf are shown in Figure 5a. In the HCl concentration range of <7 M, the K_d values of Zr and Hf are almost constant, <10 mL g^{-1}, while at the higher HCl concentration, the K_d values steeply increase to 1.5×10^4 mL g^{-1} for Zr and 4.5×10^3 mL g^{-1} for Hf at 11.5 M. This increase of the K_d value indicates that the component of the hexachloro complex of $[MCl_6]^{2-}$ adsorbed on the CA08Y resin increases with an increase of the HCl concentration. The separation factors $K_d(Zr)/K_d(Hf)$ are also plotted in Figure 5b by open diamonds. The $K_d(Zr)/K_d(Hf)$ values are 2–3 at <7 M, increase with the HCl concentration up to about 10, and again decrease to 3 at 11.5 M. The ratios of the ρ value of Zr to that of Hf, $\rho(Zr)/\rho(Hf)$, are compared in Figure 5b by closed diamonds. The $\rho(Zr)/\rho(Hf)$ value also shows a peak at around 9.5 M that comes from the difference in the onset HCl concentration for

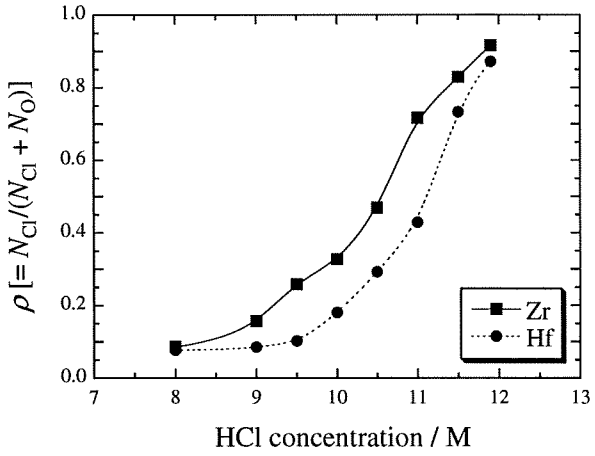

Figure 4. Variations of the ratio ρ of the N value for M–Cl ($=N_{Cl}$) to the sum of N for M–Cl and M–O ($=N_{Cl} + N_O$) as a function of the HCl concentration. The data for Zr and Hf are depicted by closed squares connected with a solid curve and closed circles with a dotted curve, respectively.

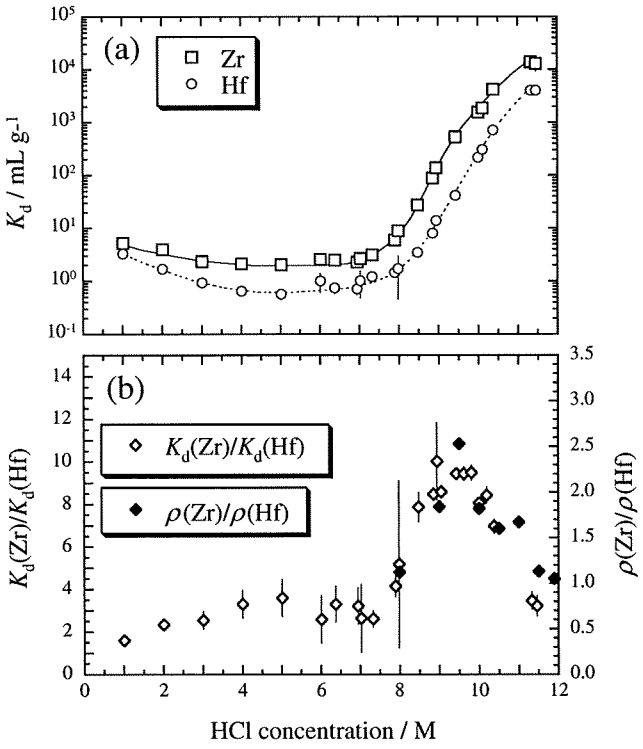

Figure 5. (a) Variations of the distribution coefficients (K_d) for Zr (open squares) and Hf (open circles) on the anion-exchange resin CA08Y as a function of the HCl concentration (Data from Ref. 10). (b) Variations of the separation factor K_d(Zr)/K_d(Hf) (open diamonds) and the ρ(Zr)/ρ(Hf) ratios (closed diamonds) as a function of the HCl concentration.

the chloride complexation of Zr and Hf (see Figure 4). It is found that the variation of the K_d values of Zr and Hf reasonably reflect the structural changes of the complexes deduced from the present EXAFS measurements.

In a previous report,[10] the adsorption probabilities (%ads) of Rf on CA08Y, which were the measure of the K_d value, were determined from 1893 cycles of anion-exchange experiments in 4.0–11.5 M HCl. The variations of the %ads values of ^{85}Zr, ^{169}Hf, and ^{261}Rf are shown as a function of the HCl concentration in Figure 6. The %ads values of Rf increase with an increase of the HCl concentration from $4.5_{-3.2}{}^{+6.3}$% at 4.0 M to $97_{-6}{}^{+3}$% at 11.5 M. This adsorption behavior of Rf is quite similar to that of Zr and Hf, and is typical of the group-4 elements. It should be also noted here that the onset HCl concentration for Rf is clearly lower than that for Zr. The anion-exchange results together with those of the EXAFS studies clearly suggest that Rf forms the same complexes as those of Zr and Hf in HCl: $[Rf(H_2O)_8]^{4+} \rightarrow [RfCl_6]^{2-}$, and that the chloride complexation of Rf is stronger than that of the homologs Zr and Hf.

Conclusion

The structural changes of Zr and Hf complexes, $[M(H_2O)_8]^{4+} \rightarrow [MCl_6]^{2-}$, were determined by EXAFS as a function of HCl concentration at 8.0–11.9 M. The onset HCl concentration for the chloride complexation of Zr is lower than

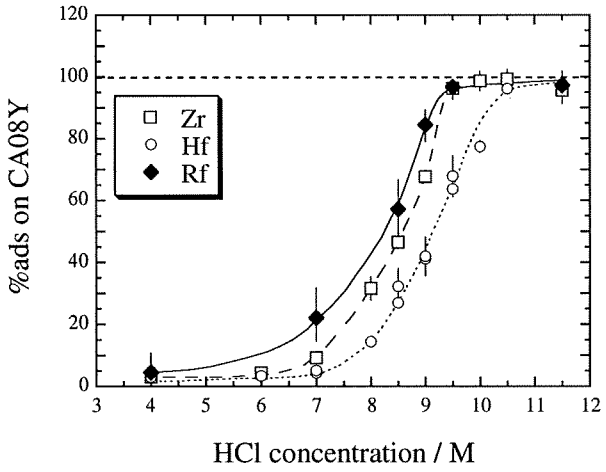

Figure 6. Variations of the adsorption probabilities (%ads) for Zr (open squares), Hf (open circles), and Rf (closed diamonds) on the anion-exchange resin CA08Y as a function of the HCl concentration (Data from Ref. 10).

that of Hf, indicating that the affinity of the Cl^- ion for Zr is stronger than that for Hf. Taking into account the anion-exchange results, it was suggested that Rf also forms the same complexes as those of Zr and Hf, $[Rf(H_2O)_8]^{4+} \rightarrow [RfCl_6]^{2-}$, and that the affinity of Cl^- for these metal ions is in the following sequence Rf > Zr > Hf.

We would like to express our gratitude to Dr. Y. Okamoto of the Japan Atomic Energy Agency for his invaluable assistance in the course of the experiment. We thank Profs. M. Nomura and Y. Inada of KEK-PF for helpful discussions on the EXAFS analyses.

References

1 *The Chemistry of Superheavy Elements*, ed. by M. Schädel, Kluwer Academic Publishers, Dordrecht, **2003**.

2 J. V. Kratz, *Pure Appl. Chem.* **2003**, *75*, 103.

3 J. V. Kratz, in *Handbook of Nuclear Chemistry*, ed. by A. Vértes, S. Nagy, Z. Klencsár, Kluwer Academic Publishers, Dordrecht, **2003**, Vol. 2, pp. 323–395.

4 M. Schädel, *Angew. Chem., Int. Ed.* **2006**, *45*, 368.

5 D. C. Hoffman, D. M. Lee, V. Pershina, in *The Chemistry of the Actinide and Transactinide Elements*, 3rd ed., ed. by L. R. Morss, N. M. Edelstein, J. Fuger, Springer, Dordrecht, **2006**, Vol. 3, pp. 1652–1752.

6 V. G. Pershina, *Chem. Rev.* **1996**, *96*, 1977.

7 P. Schwerdtfeger, M. Seth, in *Encyclopedia of Computational Chemistry*, ed. by P. v. R. Schleyer, N. L. Allinger, T. Clark, J. Gasteiger, P. A. Kollman, H. F. Schaefer, III, P. R. Schreiner, John Wiley & Sons, Chichester, **1998**, Vol. 4, pp. 2480–2499.

8 E. K. Hulet, R. W. Lougheed, J. F. Wild, J. H. Landrum, J. M. Nitschke, A. Ghiorso, *J. Inorg. Nucl. Chem.* **1980**, *42*, 79.

9 K. R. Czerwinski, K. E. Gregorich, N. J. Hannink, C. D. Kacher, B. A. Kadkhodayan, S. A. Kreek, D. M. Lee, M. J. Nurmia, A. Türler, G. T. Seaborg, D. C. Hoffman, *Radiochim. Acta* **1994**, *64*, 23.

10 H. Haba, K. Tsukada, M. Asai, S. Goto, A. Toyoshima, I. Nishinaka, K. Akiyama, M. Hirata, S. Ichikawa, Y. Nagame, Y.

Shoji, M. Shigekawa, T. Koike, M. Iwasaki, A. Shinohara, T. Kaneko, T. Maruyama, S. Ono, H. Kudo, Y. Oura, K. Sueki, H. Nakahara, M. Sakama, A. Yokoyama, J. V. Kratz, M. Schädel, W. Brüchle, *J. Nucl. Radiochem. Sci.* **2002**, *3*, 143.

11 T. Ressler, *J. Synchrotron Radiat.* **1998**, *5*, 118.

12 A. L. Ankudinov, J. J. Rehr, *Phys. Rev. B* **1997**, *56*, R1712.

13 W. P. Griffith, T. D. Wickins, *J. Chem. Soc. A* **1967**, 675.

14 J. E. D. Davies, D. A. Long, *J. Chem. Soc. A* **1968**, 2560.

15 R. C. Fay, *The Synthesis, Reactions, Properties & Applications of Coordination Compounds* in *Comprehensive Coordination Chemistry*, ed. by G. Wilkinson, R. D. Gillard, J. A. McCleverty, Pergamon Press, Oxford, **1987**, Vol. 3, pp. 363–451.

16 C. Hagfeldt, V. Kessler, I. Persson, *Dalton Trans.* **2004**, 2142.

17 G. Engel, *Z. Kristallogr.* **1935**, *90*, 341.

18 H. Schmidbaur, R. Pichl, G. Müller, *Z. Naturforsch., B: Chem. Sci.* **1986**, *41b*, 395.

19 S. I. Troyanov, V. B. Rybakov, *Koord. Khim.* **1988**, *14*, 1548.

20 E. Hartmann, K. Dehnicke, *Z. Naturforsch., B: Chem. Sci.* **1989**, *44b*, 1155.

21 K. Ruhlandt-Senge, A.-D. Bacher, U. Müller, *Acta Crystallogr., Sect. C* **1990**, *46*, 1925.

22 S. I. Troyanov, B. I. Kharisov, S. S. Berdonosov, *Russ. J. Inorg. Chem.* **1992**, *37*, 1250.

23 J. Beck, K.-J. Schlitt, *Chem. Ber.* **1995**, *128*, 763.

24 K.-H. Thiele, Ch. Schließburg, B. Neumüller, *Z. Anorg. Allg. Chem.* **1995**, *621*, 1106.

25 L. Chen, F. A. Cotton, *Inorg. Chem.* **1996**, *35*, 7364.

26 L. Chen, F. A. Cotton, W. A. Wojtczak, *Inorg. Chim. Acta* **1996**, *252*, 239.

27 J. Beck, P. Biedenkopf, K. Müller-Buschbaum, J. Richter, K.-J. Schlitt, *Z. Anorg. Allg. Chem.* **1996**, *622*, 292.

28 I. A. Guzei, L. M. Liable-Sands, A. L. Rheingold, C. H. Winter, *Z. Kristallogr.* **1998**, *213*, 221.

29 A. Baumann, J. Beck, T. Hilbert, *Z. Naturforsch., B: Chem. Sci.* **1999**, *54*, 1253.

30 E. Gauch, J. Strähle, *Z. Anorg. Allg. Chem.* **2000**, *626*, 1153.

31 J. Beck, A. Desgroseilliers, K. Müller-Buschbaum, K.-J. Schlitt, *Z. Anorg. Allg. Chem.* **2002**, *628*, 1145.

32 J. Beck, M. Kellner, M. Kreuzinger, *Z. Anorg. Allg. Chem.* **2002**, *628*, 2656.

33 C. Hagfeldt, V. Kessler, I. Persson, *New J. Chem.* **2003**, *27*, 850.

34 J. Beck, S. Hedderich, *J. Solid State Chem.* **2003**, *172*, 12.

35 A. Baumann, J. Beck, *Z. Anorg. Allg. Chem.* **2004**, *630*, 2078.

36 C. Zhong, T. Sasaki, A. Jimbo-Kobayashi, E. Fujiwara, A. Kobayashi, M. Tada, Y. Iwasawa, *Bull. Chem. Soc. Jpn.* **2007**, *80*, 2365.

37 J. Chojnacki, R. Grubba, B. Kugiel-Rachwalska, J. Pikies, *Polyhedron* **2007**, *26*, 1579.

38 R. M. Friedman, J. D. Corbett, *Inorg. Chem.* **1973**, *12*, 1134.

39 S. I. Troyanov, B. I. Kharisov, S. S. Berdonosov, *Russ. J. Inorg. Chem.* **1993**, *38*, 441.

40 B. Neumüller, K. Dehnicke, *Z. Anorg. Allg. Chem.* **2004**, *630*, 2576.

J|A|C|S
COMMUNICATIONS

Published on Web 06/10/2009

† JAEA.
‡ RIKEN.
§ Osaka University.
∥ Tokyo Metropolitan University.

10.1021/ja9030038 CCC: $40.75

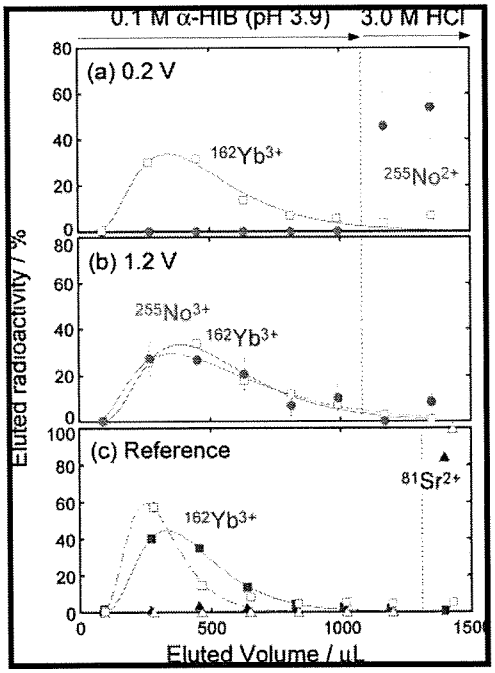

Figure 1. Elution behavior of ^{255}No and ^{162}Yb at applied potentials of (a) 0.2 and (b) 1.2 V. (c) Elution of the typical trivalent cation $^{162}Yb^{3+}$ and divalent $^{81}Sr^{2+}$ in the reference experiment, with solid symbols showing data at 0.2 V and open symbols data at 1.2 V.

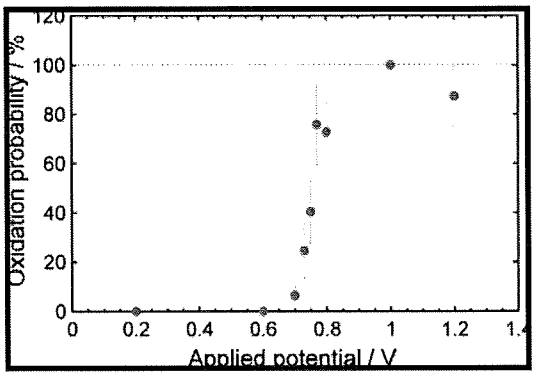

Figure 2. Oxidation probability of ^{255}No vs applied potential.

References

(1) Schädel, M. *Angew. Chem., Int. Ed.* **2006**, *45*, 368.
(2) Pershina, V. *Chem. Rev.* **1996**, *96*, 1977.
(3) (a) Pyykkö, P. *Chem. Rev.* **1988**, *88*, 563. (b) Küchle, W.; Dolg, M.; Stoll, H. *J. Phys. Chem. A* **1997**, *101*, 7128.
(4) Brüchle, W.; Schädel, M.; Scherer, U. W.; Kratz, J. V.; Gregorich, K. E.; Lee, D.; Nurmia, M.; Chasteler, R. M.; Hall, H. L.; Henderson, R. A.; Hoffman, D. C. *Inorg. Chim. Acta* **1988**, *146*, 267.
(5) Edelstein, N. M., Fuger, J., Katz, J. J., Morss, L. R. In *The Chemistry of the Actinide and Transactinide Elements*, 3rd ed.; Morss, L. R., Edelstein, N. M., Fuger, J., Eds.; Springer: Dordrecht, The Netherlands, 2006; Chapter 15, pp 1767−1768.
(6) The variations of the ionic radii of the heavy actinides and lanthanides are shown in the Supporting Information.
(7) (a) Bratsch, S. G.; Lagowski, J. J. *J. Phys. Chem.* **1986**, *90*, 307. (b) David, F. *J. Less-Common Met.* **1986**, *121*, 27.
(8) (a) Maly, J.; Sikkeland, T.; Silva, R.; Ghiorso, A. *Science* **1968**, *160*, 1114. (b) Silva, R. J.; Sikkeland, T.; Nurmia, M.; Ghiorso, A. *J. Inorg. Nucl. Chem.* **1969**, *31*, 3405.
(9) Toyoshima, A.; Kasamatsu, Y.; Kitatsuji, Y.; Tsukada, K.; Haba, H.; Shinohara, A.; Nagame, Y. *Radiochim. Acta* **2008**, *96*, 323.
(10) A cross sectional drawing of the electrochemical apparatus is shown in the Supporting Information.
(11) Haba, H.; et al. *J. Am. Chem. Soc.* **2004**, *126*, 5219.

JA9030038

4.1 Anion-exchange experiment of Db with 0.31 M HF/0.10 M HNO_3 solution

Y. Kasamatsu[1,2], A. Toyoshima[1], M. Asai[1], K. Tsukada[1], Z. Li[1], Y. Ishii[1], T.K. Sato[1], I. Nishinaka[1], T. Kikuchi[1], H. Haba[2], Y. Kudou[2], N. Sato[2], Y. Oura[3], K. Akiyama[3], K. Ooe[4], H. Fujisawa[4], A. Shinohara[5], S. Goto[5], H. Kudo[5], M. Araki[6], M. Nishikawa[6], A. Yokoyama[6] and Y. Nagame[1]

Chemical experiments of element 105 (Db), the group-5 element in the 7th period, have been performed by comparative studies with its homologues Nb and Ta and the pseudo homologue Pa [1]. Only few clear results have been, however, obtained and little is known about the chemical properties of Db. For a deeper understanding of the properties of Db, more detailed chemical investigations are required. In our previous work [2], anion-exchange behavior of Nb, Ta, and Pa in HF/HNO_3 solution was systematically investigated by a batch method, and significantly different behavior among these elements was observed. It is very interesting to explore how Db behaves in the anion-exchange chromatography. Based on the results of online anion-exchange experiments with Nb and Ta [3], we conducted the first anion-exchange experiment of Db in 0.89 M HF/0.30 M HNO_3 solution [4]. Unfortunately, the obtained distribution coefficient, K_d, was an upper limit due to the small α events of Db. In the present experiment, the anion-exchange behavior of Db in 0.31 M HF/0.10 M HNO_3 was studied by using a newly developed rapid ion-exchange and α-spectroscopy apparatus "AIDA-II" [5].

Dubnium-262 was produced in the $^{248}Cm(^{19}F, 5n)$ reaction. Reaction products were continuously transported by a He/KF gas-jet system to the collection site of AIDA-II in the chemistry laboratory. The products collected for 83 s were dissolved in 300 μL of 0.31 M HF/0.10 M HNO_3 solution ($[F^-]$ = 0.0030 M) and were fed onto the column (ϕ1.0 mm × 3.5 mm) filled with the anion-exchange resin MCl GEL CA08Y at a flow rate of 1.2 mL/min. The eluate was collected on a 15 mm × 300 mm tantalum sheet which was continuously moving toward an α-particle detection chamber at 20 mm/s (fraction 1). The sample on the sheet was automatically evaporated to dryness with a halogen heat lamp and was subjected to an α-particle measurement in the chamber equipped with an array of 12 silicon PIN photodiode detectors [5]. The remaining Db on the resin was stripped with 290 μL of 0.015 M HF/6.0 M HNO_3. The effluent was collected on another sheet and was subjected to the α-particle measurement in the same way (fraction 2). This anion-exchange cycle was repeated 1222 times.

A total of 26 α counts were detected in the energy region of interest for the decay of 34-s ^{262}Db and its daughter 3.9-s ^{258}Lr. By correcting for background α counts, the number of α counts ascribed to the decay of the nuclides was evaluated as 9.7 for fraction 1 and 7.6 for fraction 2. The percent adsorption (*%ads*) of

[1] Japan Atomic Energy Agency (JAEA)
[2] The Institute of Physical and Chemical Research (RIKEN)
[3] Tokyo Metropolitan University
[4] Niigata University
[5] Osaka University
[6] Kanazawa University

56^{+16}_{-13}% was obtained according to an equation of $\%ads = 100 \times A_2 / (A_1 + A_2)$, where A_1 and A_2 are radioactivities in the fractions 1 and 2, respectively. The K_d value of Db was evaluated from the *%ads* value with the relationship between the *%ads* values and the K_d values of Nb and Ta [3] and is plotted in Fig. 1 together with the upper limit in 0.89 M HF/0.30 M HNO_3 obtained previously [4]. It is found that the adsorption of Db on the resin in the solution with $[F^-]$ of 0.0030 M is considerably weaker than that of the closest homologue Ta in the periodic table and is similar to that of the lighter homologue Nb and the pseudo homologue Pa.

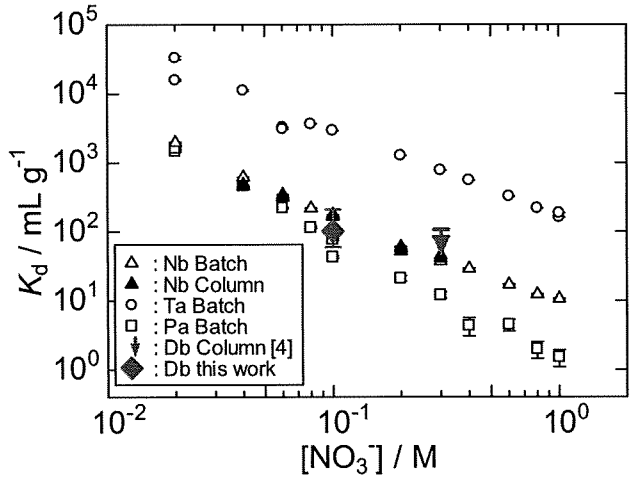

Fig. 1 K_d values of Nb, Ta, Pa, and Db as a function of $[NO_3^-]$ at constant $[F^-]$ of 0.0030 M.

References

[1] J. V. Kratz, The Chemistry of Superheavy Elements, Kluwer Academic Publishers, Dordrecht (2003) 175-191.

[2] Y. Kasamatsu *et al.*, J. Radioanal. Nucl. Chem. 279 (2009) 361-367.

[3] Y. Kasamatsu *et al.*, JAEA-Review 2007-046 (2008) 65-66.

[4] Y. Kasamatsu *et al.*, JAEA-Review 2008-054 (2008) 65-66.

[5] K. Tsukada *et al.*, JAEA-Review 2008-054 (2008) 67-68.

Anionic Fluoro Complex of Element 105, Db

Yoshitaka Kasamatsu,*[1,2] Atsushi Toyoshima,[1] Masato Asai,[1] Kazuaki Tsukada,[1] Zijie Li,[1] Yasuo Ishii,[1] Hayato Toume,[1] Tetsuya K. Sato,[1] Takahiro Kikuchi,[1] Ichiro Nishinaka,[1] Yuichiro Nagame,[1] Hiromitsu Haba,[2] Hidetoshi Kikunaga,[2] Yuki Kudou,[2] Yasuji Oura,[3] Kazuhiko Akiyama,[3] Wataru Sato,[4] Kazuhiro Ooe,[4] Hiroyuki Fujisawa,[4] Atsushi Shinohara,[4] Shin-ichi Goto,[5] Taichi Hasegawa,[5] Hisaaki Kudo,[5] Tomohiro Nanri,[6] Mikio Araki,[6] Norikazu Kinoshita,[6] Akihiko Yokoyama,[7] Fangli Fan,[8] Zhi Qin,[8] Christoph E. Düllmann,[9] Matthias Schädel,[9] and Jens V. Kratz[10]

[1]*Advanced Science Research Center, Japan Atomic Energy Agency, Tokai, Naka-gun, Ibaraki 319-1195*

[2]*Nishina Center for Accelerator Based Science, RIKEN, Wako 351-0198*

[3]*Graduate School of Science and Engineering, Tokyo Metropolitan University, Hachioji, Tokyo 192-0397*

[4]*Graduate School of Science, Osaka University, Toyonaka, Osaka 560-0043*

[5]*Faculty of Science, Niigata University, Niigata 950-2181*

[6]*Graduate School of Natural Science and Technology, Kanazawa University, Kanazawa 920-1192*

[7]*Institute of Science and Engineering, Kanazawa University, Kanazawa 920-1192*

[8]*Institute of Modern Physics, Chinese Academy of Science, Lanzhou 730000, P. R. China*

[9]*GSI Helmholtzzentrum für Schwerionenforschung GmbH, D-64291 Darmstadt, Germany*

[10]*Institut für Kernchemie Universität Mainz, D-55099 Mainz, Germany*

(Received August 27, 2009; CL-090785; E-mail: kasamatsu@riken.jp)

We report on the characteristic anion-exchange behavior of the *superheavy* element dubnium (Db) with atomic number $Z = 105$ in HF/HNO_3 solution at the fluoride ion concentration $[F^-] = 0.003$ M. The result clearly demonstrates that the fluoro complex formation of Db is significantly different from that of the group-5 homologue Ta in the 6th period of the periodic table while the behavior of Db is similar to that of the lighter homologue Nb in the 5th period.

Transactinide elements (superheavy elements) with $Z \geq 104$ are produced at accelerators using heavy-ion-induced nuclear reactions. Because of their low production rates and short half-lives, chemical experiments with these elements must be performed on a one-atom-at-a-time scale. Thus, chemical characterization of these elements at the uppermost end of the periodic table is extremely challenging as well as fascinating.[1] In the past, the chemical behavior of Db, the group-5 element in the 7th period of the periodic table, in aqueous phases has been investigated using the nuclides ^{262}Db ($T_{1/2} = 34$ s) and ^{263}Db ($T_{1/2} = 27$ s) by comparison with each behavior of the lighter homologues, Nb and Ta, and also of the pentavalent pseudo-homologue Pa.[1,2] Little is, however, known about the chemical properties of Db because of the constraint of one-atom-at-a-time experiments.

In our previous work,[3] the anion-exchange behavior of Db in 13.9 M HF solution was studied with the rapid chemical separation apparatus AIDA with which the anion- and cation-exchange behavior of element 104 (Rf) in HF and HF/HNO_3 solutions was successfully investigated.[4–6] It was found that the distribution coefficient (K_d) of Db is smaller than those of Nb and Ta that presumably form $[MF_6]^-$ and/or $[MF_7]^{2-}$ (M = Nb and Ta) in 13.9 M HF. The behavior of Db was also compared with that of Pa for reference. While the K_d values of these anionic fluoro complexes on the resin decreases in the sequence of Ta $\approx$ Nb > Db $\geq$ Pa, the chemical species of Db was not determined. In solutions with more dilute fluoride ion concentration $[F^-]$, Nb is known to form fluoro–oxo complexes, whereas Ta forms fluoro complexes.[7] In fact, we have ascertained the significantly different anion-exchange behavior between Nb and Ta in the HF/HNO_3 mixed solution ($[F^-] \leq 0.01$ M);[8] see Figure 1. It is, therefore, of great interest to explore how Db behaves in anion-exchange chromatography in the dilute $[F^-]$ solution. In this report, we present a successful measurement of the K_d value of Db in 0.31 M HF/0.10 M HNO_3 solution ($[F^-] = 0.003$ M), where Nb and Ta form $[NbOF_4]^-$ and $[TaF_6]^-$, respectively,[7,8] and briefly discuss the chemical form of Db.

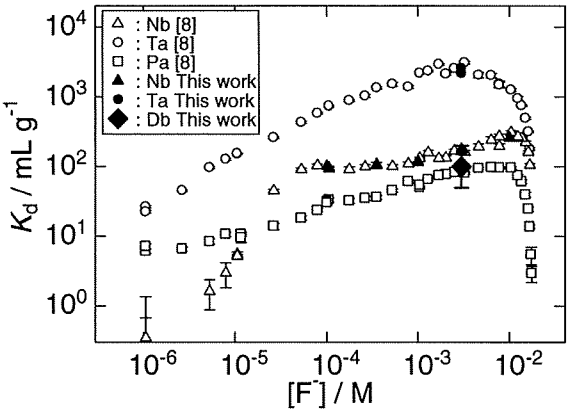

Figure 1. Distribution coefficients, K_d, of Nb, Ta, Pa, and Db on the anion-exchange resin in HF/0.1 M HNO_3 depending on the fluoride ion concentration.

Dubnium-262 was produced in the ^{248}Cm(^{19}F, 5*n*) reaction with a production rate of about 0.5 atoms per min at the JAEA tandem accelerator.[9] The beam energy ranged from 102.1 to 103.8 MeV in the ^{248}Cm target (1.4 mg cm^{-2}), and the average beam current was 440 particle nA. Reaction products recoiling out of the target were continuously transported by a He/KF gas-jet system from the target chamber to the collection site of the newly developed rapid ion-exchange apparatus located in the chemistry laboratory.[10] After collection for 83.4 s, the products were dissolved in 300 μL of 0.31 M HF/0.10 M HNO_3 and subsequently fed onto the microcolumn (1.0-mm i.d. × 3.5-mm long) filled with the anion-exchange resin MCI GEL CA08Y (particle size of 25 μm) at a flow rate of 1.2 mL min^{-1}. The elu-

ate was collected as Fraction 1 on a 15 × 300-mm tantalum sheet (0.15-mm thickness) which was continuously moving toward an α-particle detection chamber at 2.0 cm s^{-1}. The sample on the sheet was automatically evaporated to dryness with a halogen heat lamp and then subjected to the α-particle measurement for 75 s in the chamber equipped with an array of 12 silicon PIN photodiodes.[10] Remaining products on the resin were stripped with 290 μL of 0.015 M HF/6.0 M HNO_3. The eluate was collected on another Ta sheet as Fraction 2 followed by the same procedures for sample preparation and measurement. The α-particle measurement was started 14 and 38 s after the end of product collection for Fractions 1 and 2, respectively. The above procedure was repeated 1222 times. In the ^{248}Cm target, Gd (39%-enriched ^{152}Gd) was admixed to simultaneously produce ^{169}Ta through the Gd(^{19}F, *xn*) reactions. After the α-particle measurement, the samples on the sheets were assayed by γ-ray spectrometry with a Ge detector to monitor the transport efficiency of the gas-jet system and to determine the chemical yield and the adsorption behavior of ^{169}Ta. In separate experiments, the nuclides ^{90}Nb and ^{178m}Ta were produced in the Zr/Hf(*p*, *xn*) reactions, and ^{88}Nb and ^{170}Ta were produced in the Ge/Gd(^{19}F, *xn*) reactions. Then, the anion-exchange behavior of Nb and Ta was studied in the same way as that for Db. Elution curves of the nuclides were obtained by γ-ray spectrometry for eluate fractions.

α-Particle energies of ^{262}Db and its daughter nuclide ^{258}Lr ($T_{1/2} = 3.9$ s) are in the range from 8.3 to 8.7 MeV.[9] In this work, α events detected in the energy range of 8.1–8.7 MeV were assigned to the decays of ^{262}Db and ^{258}Lr taking into account the energy resolution of 60–150 keV in full width at half-maximum. A total of 26 α events were registered in this energy range. It should be noted that the α events in this range were almost free from interfering events originating from other products. After subtracting the background count rate of 7.5×10^{-7} counts/s for each detector, the number of α events ascribed to the decays of ^{262}Db and ^{258}Lr was 9.7 for Fraction 1 and 7.6 for Fraction 2. One time-correlated α particle pair of ^{262}Db and ^{258}Lr was also detected. The cross section of ^{262}Db was evaluated to be 1–2 nb from the α-decay events with a 30% detection efficiency, 60% chemical yield, α-decay branches of 64% for ^{262}Db and 100% for ^{258}Lr, and a 25% transport efficiency of the gas-jet system.[9] This value is in good agreement with our previously measured value of 1.5 ± 0.4 nb.[3,9]

The adsorption probability (*%ads*) of Db on the resin was determined to be 56^{+16}_{-13}% from the α-decay counts detected in both Fractions 1 and 2. The asymmetric error limits were evaluated from the counting statistics of the observed α events at the 68% confidence level for Poisson distributed variables.[11] The *%ads* values of Nb and Ta under the same conditions as for Db were evaluated from their elution curves to be 76 ± 2% and >99%, respectively. The K_d values of Nb and Ta were also determined from their elution curves,[4,5] and the values agree well with those from the previous batchwise experiment[8] as shown in Figure 1. This indicates that chemical equilibrium is reached in the fluoride complexation and ion-exchange process of these elements under the present conditions. The K_d value of Db plotted in Figure 1 was evaluated from its *%ads* in the same way as described in refs 4 and 5. It is found that the adsorption of Db on the resin is considerably weaker than that of Ta and is similar to that of Nb and also Pa. From the discussion on the fluoro complexes of the group-5 elements based on their K_d values,[8] the present result suggests that Db would form an fluoro–oxo complex $[DbOF_4]^-$ like Nb, but not $[DbF_6]^-$ like Ta. Note that the K_d value of Db is also close to that of Pa that forms $[PaOF_5]^{2-}$ and/or $[PaF_7]^{2-}$.[8,12,13] Formation of complexes with the −2 charge state such as $[DbOF_5]^{2-}$ and $[DbF_7]^{2-}$ could be suggested for Db. To unequivocally clarify the fluoride complexation of Db, further systematic study of Db as a function of $[F^-]$ and $[NO_3^-]$ is required.

References and Notes

1 M. Schädel, *Angew. Chem., Int. Ed.* **2006**, *45*, 368.
2 W. Paulus, J. V. Kratz, E. Strub, S. Zauner, W. Brüchle, V. Pershina, M. Schädel, B. Schausten, J. L. Adams, K. E. Gregorich, D. C. Hoffman, M. R. Lane, C. Laue, D. M. Lee, C. A. McGrath, D. K. Shaughnessy, D. A. Strellis, E. R. Sylwester, *Radiochim. Acta* **1999**, *84*, 69, and references therein.
3 K. Tsukada, H. Haba, M. Asai, A. Toyoshima, K. Akiyama, Y. Kasamatsu, I. Nishinaka, S. Ichikawa, K. Yasuda, Y. Miyamoto, K. Hashimoto, Y. Nagame, S. Goto, H. Kudo, W. Sato, A. Shinohara, Y. Oura, K. Sueki, H. Kikunaga, N. Kinoshita, A. Yokoyama, M. Schädel, W. Brüchle, J. V. Kratz, *Radiochim. Acta* **2009**, *97*, 83.
4 H. Haba, K. Tsukada, M. Asai, A. Toyoshima, K. Akiyama, I. Nishinaka, M. Hirata, T. Yaita, S. Ichikawa, Y. Nagame, K. Yasuda, Y. Miyamoto, T. Kaneko, S. Goto, S. Ono, T. Hirai, H. Kudo, M. Shigekawa, A. Shinohara, Y. Oura, H. Nakahara, K. Sueki, H. Kikunaga, N. Kinoshita, N. Tsuruga, A. Yokoyama, M. Sakama, S. Enomoto, M. Schädel, W. Brüchle, J. V. Kratz, *J. Am. Chem. Soc.* **2004**, *126*, 5219.
5 A. Toyoshima, H. Haba, K. Tsukada, M. Asai, K. Akiyama, S. Goto, Y. Ishii, I. Nishinaka, T. K. Sato, Y. Nagame, W. Sato, Y. Tani, H. Hasegawa, K. Matsuo, D. Saika, Y. Kitamoto, A. Shinohara, M. Ito, J. Saito, H. Kudo, A. Yokoyama, M. Sakama, K. Sueki, Y. Oura, H. Nakahara, M. Schädel, W. Brüchle, J. V. Kratz, *Radiochim. Acta* **2008**, *96*, 125.
6 Y. Ishii, A. Toyoshima, K. Tsukada, M. Asai, H. Toume, I. Nishinaka, Y. Nagame, S. Miyashita, T. Mori, H. Suganuma, H. Haba, M. Sakamaki, S. Goto, H. Kudo, K. Akiyama, Y. Oura, H. Nakahara, Y. Tashiro, A. Shinohara, M. Schädel, W. Brüchle, V. Pershina, J. V. Kratz, *Chem. Lett.* **2008**, *37*, 288.
7 O. L. Keller, A. Chethan-Strode, *Inorg. Chem.* **1966**, *5*, 367.
8 Y. Kasamatsu, A. Toyoshima, H. Haba, H. Toume, K. Tsukada, K. Akiyama, T. Yoshimura, Y. Nagame, *J. Radioanal. Nucl. Chem.* **2009**, *279*, 371, and references therein.
9 Y. Nagame, M. Asai, H. Haba, S. Goto, K. Tsukada, I. Nishinaka, K. Nishio, S. Ichikawa, A. Toyoshima, K. Akiyama, H. Nakahara, M. Sakama, M. Schädel, J. V. Kratz, H. W. Gäggeler, A. Türler, *J. Nucl. Radiochem. Sci.* **2002**, *3*, 85.
10 K. Tsukada, Y. Kasamatsu, M. Asai, A. Toyoshima, Y. Ishii, H. Toume, Y. Nagame, *JAEA-Rev. 2008-054* **2008**, p. 67.
11 W. Brüchle, *Radiochim. Acta* **2003**, *91*, 71.
12 *The Chemistry of the Actinide and Transactinide Elements*, 3rd ed., ed. by L. R. Morss, N. M. Edelstein, J. Fuger, Springer, Dordrecht. **2006**, Vol. 1, Chap. 4, pp. 212–218.
13 M. V. Di Giandomenico, C. Le Naour, E. Simoni, D. Guillaumont, Ph. Moisy, C. Hennig, S. D. Conradson, C. Den Auwer, *Radiochim. Acta* **2009**, *97*, 347.

Published on the web (Advance View) October 17, 2009; doi:10.1246/cl.2009.1084

Half-life estimation of the first excited state of ^{229}Th by using α-particle spectrometry

H. Kikunaga,[1,2,*] Y. Kasamatsu,[3] H. Haba,[2] T. Mitsugashira,[4] M. Hara,[5] K. Takamiya,[6] T. Ohtsuki,[7] A. Yokoyama,[8] T. Nakanishi,[8] and A. Shinohara[1]

[1]*Graduate School of Science, Osaka University, Toyonaka, Osaka 560-0043, Japan*
[2]*Nishina Center for Accelerator-Base Science, RIKEN, Wako, Saitama 351-0198, Japan*
[3]*Advanced Science Research Center, Japan Atomic Energy Agency, Tokai, Ibaraki 319-1195, Japan*
[4]*Institute for Material Research, Tohoku University, Sendai, Miyagi 980-8577, Japan*
[5]*International Research Center for Nuclear Materials Science, Tohoku University, Oarai-machi, Ibaraki 311-1313, Japan*
[6]*Research Reactor Institute, Kyoto University, Kumatori, Osaka 590-0494, Japan*
[7]*Laboratory of Nuclear Science, Tohoku University, Sendai, Miyagi 982-0826, Japan*
[8]*Graduate School of Natural Science and Technology, Kanazawa University, Kanazawa, Ishikawa 920-1192, Japan*

(Received 22 May 2009; published 21 September 2009)

To search for a direct-decay signal from the isomer ^{229}Th^m, α-particle spectra of ^{229}Th^{m,g} produced from 93 mg of ^{233}U have been measured by using a rapid and high-resolution α-particle spectrometry, which can distinguish α lines of ^{229}Th^m from those of its ground state. Although α events were not obtained in the expected energy region for ^{229}Th^m with the exception of those derived from ^{229}Th^g, we can estimate that the half-life of ^{229}Th^m is shorter than 2 h at 3σ confidence level under the chemical condition of chloride or hydroxide.

DOI: 10.1103/PhysRevC.80.034315 PACS number(s): 21.10.Tg, 23.35.+g, 23.60.+e, 27.90.+b

I. INTRODUCTION

The first excited state of ^{229}Th (^{229}Th^m) is a very interesting nuclear isomer. A number of decay studies of ^{233}U have shown that ^{229}Th^m has the excitation energy of several electron volts [1–4]. Because of its extremely low energy comparable with the binding energy of valence electrons, the half-life of ^{229}Th^m is expected to vary with the interaction between the nucleus and its orbital electron [5]. Therefore, the half-life reflects not only the nuclear structure but also its chemical environments.

The values of the half-lives of ^{229}Th^m obtained in previous researches [6,7] appeared to be inconsistent. The first experimental data of the half-life was reported by Browne *et al.* [6] in 2001. Based on γ-ray spectrometry, they searched for the growth components on the ground state of ^{229}Th (^{229}Th^g) from ^{229}Th^m using approximately 25 g of ^{233}U. From unsuccessful observation of such growth, they concluded that the ^{229}Th^m half-life should be <6 h or >20 d in 2 M HCl. In our previous works [7,8], we attempted to produce ^{229}Th^m in nuclear reactions and to measure its half-life by α-particle spectrometry. Although a sufficient quantity of counting statistics was not obtained, the half-life of ^{229}Th^m in fluoride was estimated to be 13.9 ± 3 h [7]. More accurate determination of the half-life of ^{229}Th^m would improve the experimental design for measuring its nuclear processes including direct photon emission from ^{229}Th^m [9].

The previous studies indicate that the half-life of ^{229}Th^m is around several hours or less and hence we have optimized our experiment to measure the half-life below one day. In this study, we used α-particle spectrometry to estimate the half-life of ^{229}Th^m produced from the α decay of ^{233}U whereas ^{229}Th^m was produced in nuclear reactions in our previous works. The detailed characteristics of the α decay of ^{233}U are well known and the data up to 1996 are summarized in Ref. [10]. More recent data have been presented by Barci *et al.* [2], who investigated the nuclear level scheme of ^{229}Th in detail by γ-ray spectrometry. These data indicate that the ground state of ^{233}U, assigned as the $5/2^+[633]$ Nilsson state, decays to the ground state of ^{229}Th, $5/2^+[633]$, with the branching ratio of about 87%. All the rest decay to the excited states of ^{229}Th, so that higher than 2.1% [11] of the total decay of ^{233}U is expected to decay via the level of ^{229}Th^m, $3/2^+[631]$. Therefore, the initial α-particle spectrum of ^{229}Th separated from ^{233}U is expected on the assumption that the sample consists of 98% of ^{229}Th^g and 2% of ^{229}Th^m as shown in Fig. 1. The solid line shows the spectrum of ^{229}Th^g estimated from Ref. [10] and the dashed line shows the ^{229}Th^g spectrum with the component of ^{229}Th^m estimated by Dykhne and Tkalya [11] on the assumption that the transition from ^{229}Th^m to ^{229}Th^g is negligible. The transition from ^{229}Th^m to the 149.96-keV level, $3/2^+[631]$, of ^{225}Ra is expected to be the favored α decay, whereas ^{229}Th^g decays mainly to the 236.25-keV level, $5/2^+[633]$, and has α branching of 0.16% [10] to the 149.96-keV level of ^{225}Ra. There is a large difference between those spectra in the energy region around 4930 keV. Note that the difference would be detected even if ^{229}Th^m has such a long life as not to distinguish the signal from ^{229}Th^m by a radioactive decay or growth [6,7]. Moreover, it is possible to estimate the half-life even if the difference is not observed because of a short life, because the initial amount of ^{229}Th^m is able to be estimated from that of ^{233}U. Therefore, comparing the high-resolution spectrum of "freshly" isolated ^{229}Th^{m,g} from ^{233}U with the spectrum of ^{229}Th^g is efficient for estimation of the half-life of ^{229}Th^m. The method of rapid source preparation for high-resolution α-particle spectrometry [12] has been applied to the present study.

*hkiku@chem.sci.osaka-u.ac.jp

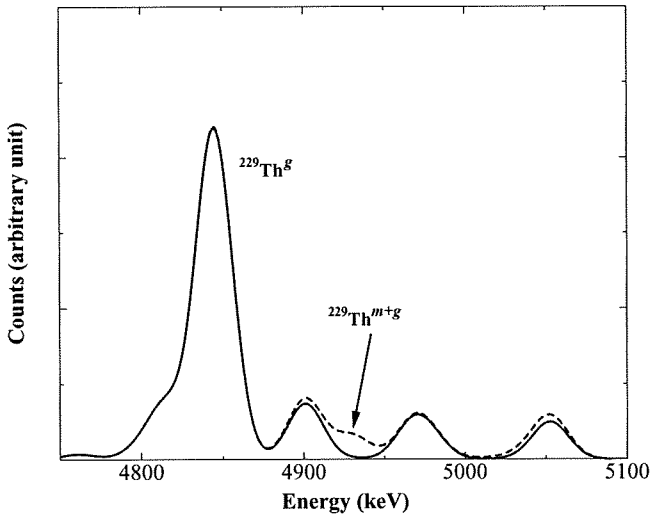

FIG. 1. Expected spectrum for fresh ^{229}Th produced from α decay of ^{233}U.

II. EXPERIMENTAL PROCEDURES

For the purification of the ^{233}U sample, we carried out an anion-exchange procedure. The U_3O_8 sample containing 93 mg of ^{233}U was supplied from the International Research Center for Nuclear Materials Science, Tohoku University. Generally, a ^{233}U sample contains ^{232}U produced in subnuclear reactions as an impurity. The ^{233}U sample used in this experiment contains 3.17 ppm of ^{232}U. The oxide sample of ^{233}U was dissolved in 12 M HCl and then precipitated by adding 15 M NH_4OH as ammonium diuranate. After a centrifugal separation, the precipitate was dissolved in 10 mL of 12 M HCl and the solution was passed through an anion-exchange column [Muromac(R) 1 × 8, 200–400 mesh, 8 mmϕ × 50 mm], which adsorbed uranium. The resin adsorbing uranium was washed with 25 mL of 9 M HCl to eliminate thorium. The uranium was eluted from the column with 10 mL of 2 M HCl and precipitated by adding 15 M NH_4OH as ammonium diuranate. The precipitate was separated from the supernatant by centrifugation. This purification was repeated three times.

The precipitate of ammonium diuranate was dissolved in 10 mL of 12 M HCl and then the solution was passed through an anion-exchange column [Muromac(R) 1 × 8, 200–400 mesh, 8 mmϕ × 50 mm] to adsorb uranium. The resin was washed with 15 mL of 9 M HCl to eliminate thorium, and then the column was left to stand for 1 h to allow the growth of ^{229}Th^{m,g}. These fresh thorium isotopes were eluted from the column with 5 mL of 9 M HCl and the eluate was passed through another anion-exchange column [Muromac(R) 1 × 8, 200–400 mesh, 8 mmϕ × 50 mm] to eliminate traces of ^{233}U from the thorium fraction. The thorium isotopes were coprecipitated with samarium hydroxide by adding 20 μg of samarium and 15 M NH_4OH in this order. The precipitate was collected on a 0.02-μm alumina filter (Whatman, ANODISC membrane) 18 mm in diameter to prepare a counting source [12]. The filter was fixed on a stainless-steel supporting ring and dried on a hot plate at 150°C. The sample was subjected to α-particle spectrometry as described below.

The accumulation for an α-particle spectrum for 600 s was repeated 20 times. The elapsed time from the elution of thorium to the start of measurement was about 15 min. After the above procedure for elution of ^{229}Th^{m,g} was performed 3 times, the ^{233}U atoms were eluted from the column with 20 mL of 2 M HCl, and again absorbed to a new column to avoid the leak of ^{233}U. The whole procedure was performed 9 times, so that a total of 27 α sources were measured.

The α-particle spectrometry was performed by using a SILENA Model 7937/*B* α-particle spectrometer and a 2048-channel pulse-height analyzer system assisted by a personal computer. The α-particle spectrometer was equipped with an ion-implanted planar silicon detector (Canberra, PD450-17-100AM). A counting source was placed at a distance of 3 cm from the detector and the counting efficiency was 3.4%.

III. RESULTS AND DISCUSSIONS

An α-particle spectrum obtained as the sum of the 27-sample spectra measured for the first 6000 s is shown in Fig. 2. The α peaks of ^{229}Th, ^{228}Th, and the daughters of ^{228}Th are seen in the spectrum. The ^{228}Th peak at 5423 keV has a full width at half maximum (FWHM) of about 25 keV. This resolution is sufficient to distinguish between α lines of ^{229}Th^{m} and those of ^{229}Th^{g}.

A magnification of the α-particle spectrum in Fig. 2 for the region related to ^{229}Th is shown in Fig. 3. The solid circles show a spectrum measured for the first 6000 s, and the open circles show a spectrum measured for the next 6000 s. The solid line shows a ^{229}Th^{g} spectrum estimated from the region of the main peak of ^{229}Th^{g}, which does not contain the component of ^{229}Th^{m}, and the linear background continuum. The component in the low-energy side of ^{229}Th is due to ^{233}U that passed through the anion-exchange column. From 1 h growth of ^{229}Th in a 93 mg sample of ^{233}U and using 27 such samples, we estimate 1800 counts due to ^{229}Th^{g} in an α spectrum measured with 3.4% efficiency for 6000 s.

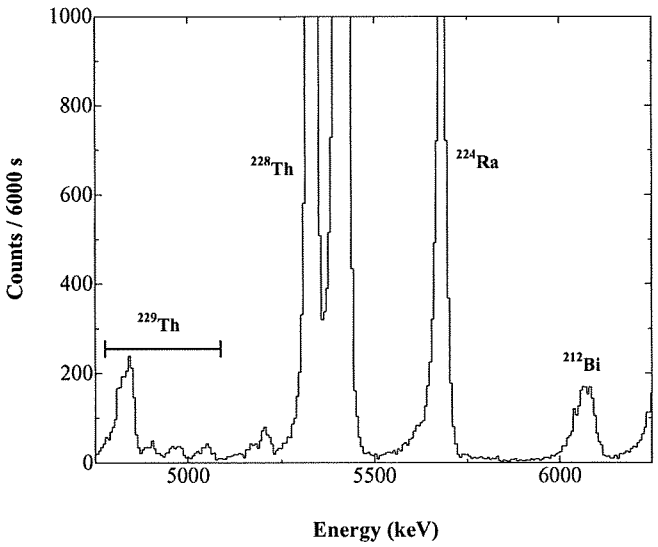

FIG. 2. An α-particle spectrum obtained as the sum of 27 spectra measured during the initial 6000 s.

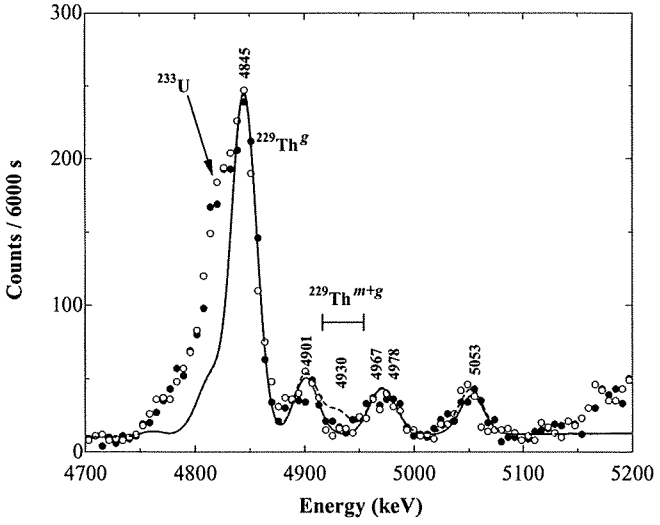

FIG. 3. A magnification of the α-particle spectrum for the region related to ^{229}Th. The solid circles show counts per channel for the initial 6000 s and the open circles show counts per channel for the following 6000 s. The lines drawn in the figures are the same as those in Fig. 1 (see text for detail).

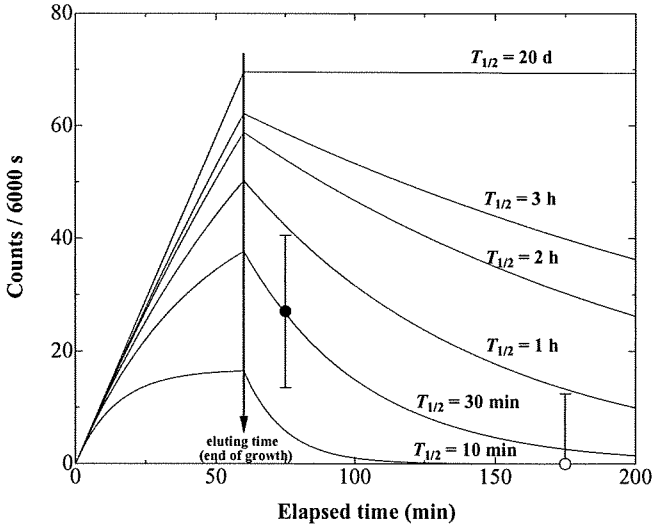

FIG. 4. Estimated growth curves in α counts in the energy region of the ^{229}Th^m α particle. Each of the six solid curves represents the expected counts of ^{229}Th^m with a half-life between 10 min and 20 d. The solid and open circles indicate the ^{229}Th^m α counts of the spectrum measured for the initial 6000 s and those for the following 6000 s, respectively.

By contrast, obtained counts of ^{229}Th^g were 1700 counts per 6000 s. The obtained counts are compatible with the expected counts considering the chemical yield in purification procedures. The ratio of the α counts of ^{229}Th^g/^{228}Th was about 1/30, which is consistent with the ratio of the α counts of ^{229}Th^g ($T_{1/2}$ = 7880 y [13]) and ^{228}Th ($T_{1/2}$ = 1.9116 y [10]) estimated from the ^{233}U ($T_{1/2} = 1.592 \times 10^5$ y [10]) atoms containing the ^{232}U ($T_{1/2}$ = 68.9 y [10]) atoms at 3.17 ppm. The dashed line shows a spectrum that is the sum of the solid line and 2% of ^{229}Th^m as well as Fig. 1. Assuming that ^{229}Th^m is stable for isomeric transition or that it has a half-life longer than a few days, one expects to obtain a spectrum corresponding with the dashed line. However, the obtained spectrum is close to the solid line, which indicates that ^{229}Th^m scarcely remained at the measurement.

To estimate the half-life of ^{229}Th^m, in Fig. 4 we show the α counts in the region of 4915–4955 keV (hereinafter called the ROI, region of interest), where the main peak of ^{229}Th^m is expected to appear, as a function of elapsed time. As with Fig. 3, the solid and open circles indicate the ROI counts of the spectrum measured for the first 6000 s and for the next 6000 s, respectively. The solid lines show the growth curves of the ROI counts with various half-life values expected as described below. Thorium isotopes were eluted from the anion-exchange column adsorbing ^{233}U at the time when the curves turn off. Until this time, ^{229}Th^{m,g} increase because of the decay of ^{233}U, and the number of atoms is given by the following equations:

$$N_m(t) = \frac{\lambda_{233}}{\lambda_m - \lambda_{233}} N_{233} \mathrm{br}_m (e^{-\lambda_{233} t} - e^{-\lambda_m t}), \quad (1)$$

$$N_g(t) = \frac{\lambda_{233}}{\lambda_g - \lambda_{233}} N_{233}(1 - \mathrm{br}_m)(e^{-\lambda_{233} t} - e^{-\lambda_g t}) + \frac{\lambda_m}{\lambda_g - \lambda_m} N_m (e^{-\lambda_m t} - e^{-\lambda_g t}), \quad (2)$$

where N_m, N_g, and N_{233} are the numbers of ^{229}Th^m, ^{229}Th^g, and ^{233}U atoms, respectively, λ_m, λ_g, and λ_{233} are the decay constants of ^{229}Th^m, ^{229}Th^g, and ^{233}U, respectively, and br$_m$ is the branching ratio of the decay of ^{233}U via ^{229}Th^m. And then the ^{229}Th^m component disintegrates to ^{229}Th^g according to its half-life. Here, the ROI counts are given by

$$\text{ROI counts} = \text{eff}\left\{I_m \lambda_{m\alpha} N_m(t) + I_g \lambda_g N_g(t)\right\} + \text{BKG}, \quad (3)$$

where eff is the total efficiency, which is 3.4% in this case, I_m and I_g are the intensities of ^{229}Th^m and ^{229}Th^g in the ROI region, respectively, $\lambda_{m\alpha}$ is the partial α-decay constant of ^{229}Th^m, and BKG is the constant-background counts in the ROI region. The partial half-life of α decay of ^{229}Th^m is estimated to be 2000 y from Refs. [7,11]. According to Refs. [10,11], the ratio of I_m to I_g is 22.8 : 1. The value of eff$\{\lambda_g N_g(t)\}$ + BKG is fitted to the solid line in Fig. 3. Although the first observed value is reproduced most likely with the curve for a half-life of 30 min, no influence of ^{229}Th^m is observed on the second value. The 3σ confidence level of both values gives an upper limit of 2 h for the half-life of ^{229}Th^m. The result is consistent with the upper limit of the short-lived case in Ref. [6], namely, 6 h.

We note that the half-life of ^{229}Th^m may change depending on its chemical form. In this study, the ^{229}Th atoms formed chloride complexes before the α-source preparation and then hydroxides for α-particle spectrum accumulation. Therefore, the present results show the half-life of ^{229}Th^m is less than 2 h under the chemical condition of at least either chloride or hydroxide.

In the framework of a single-particle transition model, the radioactive transition probability via direct photon emission is

given by the following equation:

$$\lambda = \frac{\ln 2}{T_{1/2}} = \frac{8\pi(L+1)}{L[(2L+1)!!]^2} E_\gamma^{2L+1} B(ML), \quad (4)$$

where $T_{1/2}$ is the half-life of a nuclear transition, L is the multipolarity, E_γ is an excited energy of a level, and $B(ML)$ is the reduced transition probability of the nucleus. The excitation energies of ^{229}Th^m were reported to be 3.5 ± 1.0 eV [1], 3.4 ± 1.8 eV [2], 5.5 ± 1.0 eV [3], and 7.6 ± 0.5 eV [4]. However, the reduced transition probability of ^{229}Th^m to ^{229}Th^g, $B(M1; +3/2 \rightarrow +5/2)$, was estimated to be 0.043 μ_N^2 [2]. Hence, the partial half-life of ^{229}Th^m for direct photon emission is estimated to be between 29 min and 16 h in the energy range from 2.5 to 8.1 eV in a vacuum in the framework of a single-particle transition model.

The partial half-life of less than 2 h corresponds to the excitation energy of higher than 5 eV. Therefore, if the excitation energy of ^{229}Th^m is lower than 5 eV, for example, 3.5 eV as reported in Ref. [1], the present results suggest that ^{229}Th^m should decay via not only the direct photon emission but also other decay channels, such as an electron bridge mechanism [14] and a medium effect [5]. In contrast, assuming that the excitation energy of ^{229}Th^m is larger than 5 eV, the obtained limit of the half-life of ^{229}Th^m can be explained even if the decay occurs only via the direct photon emission. In other words, the half-life of ^{229}Th^m should be shorter than 2 h regardless of the chemical forms of Th for this excitation energy. In particular, if the excitation energy is larger than an electron-binding energy of the outer valence molecular orbital of Th and its compounds, the internal conversion process is possible and the half-life is not to be significantly changed by the variation of chemical form; therefore, the half-live of shorter than 6 h [6] gives agreement with the present results whereas those of longer than 20 d [6] and 13.9 ± 3 h [7] fall outside of the limits of the results.

In conclusion, we have searched for the α events from ^{229}Th^m produced from 93 mg of ^{233}U by α-particle spectrometry with rapid source preparation. From the upper limit of such events, it was concluded that the half-life of ^{229}Th^m may be less than 2 h. The excitation energy is strongly expected to be determined more accurately by direct photon emission. If one attempts to detect the photon of isomeric transition from ^{229}Th^m with excitation energy higher than the electron-binding energy of Th compounds, as the most recent value 7.6 ± 0.5 eV [4], the experimental design for it should be based on the assumption that ^{229}Th^m has a half-life shorter than a few hours.

ACKNOWLEDGMENTS

This study was carried out under the Cooperative Research Program of the International Research Center for Nuclear Materials Science, Institute for Materials Research (IMR), Tohoku University.

[1] R. G. Helmer and C. W. Reich, Phys. Rev. C **49**, 1845 (1994).
[2] V. Barci, G. Ardisson, G. Barci-Funel, B. Weiss, O. El Samad, and R. K. Sheline, Phys. Rev. C **68**, 034329 (2003).
[3] Z. O. Guimarães-Filho and O. Helene, Phys. Rev. C **71**, 044303 (2005).
[4] B. R. Beck, J. A. Becker, P. Beiersdorfer, G. V. Brown, K. J. Moody, J. B. Wilhelmy, F. S. Porter, C. A. Kilbourne, and R. L. Kelley, Phys. Rev. Lett. **98**, 142501 (2007).
[5] E. V. Tkalya, Phys. Usp. **46**, 315 (2003).
[6] E. Browne, E. B. Norman, R. D. Canaan, D. C. Glasgow, J. M. Keller, and J. P. Young, Phys. Rev. C **64**, 014311 (2001).
[7] T. Mitsugashira, M. Hara, T. Ohtsuki, H. Yuki, K. Takamiya, Y. Kasamatsu, A. Shinohara, H. Kikunaga, and T. Nakanishi, J. Radiol. Nucl. Chem. **255**, 63 (2003).
[8] H. Kikunaga, Y. Kasamatsu, K. Takamiya, T. Mitsugashira, M. Hara, T. Ohtsuki, H. Yuki, A. Shinohara, S. Shibata, N. Kinoshita, A. Yokoyama, and T. Nakanishi, Radiochim. Acta **93**, 507 (2005).
[9] Y. Kasamatsu, H. Kikunaga, K. Takamiya, T. Mitsugashira, T. Nakanishi, Y. Ohkubo, T. Ohtsuki, W. Sato, and A. Shinohara, Radiochim. Acta **93**, 511 (2005).
[10] R. B. Firestone and V. S. Shirley, Eds., *Table of Isotopes*, 8th ed. (Wiley & Sons, New York, 1996).
[11] A. M. Dykhne and E. V. Tkalya, JETP Lett. **67**, 251 (1998).
[12] H. Kikunaga, Y. Kasamatsu, K. Takamiya, T. Ohtsuki, H. Yuki, A. Yokoyama, T. Nakanishi, and T. Mitsugashira, Appl. Radiat. Isot. **67**, 539 (2009).
[13] S. J. Goldstein, M. T. Murrell, and R. W. Williams, Phys. Rev. C **40**, 2793 (1989).
[14] D. Hinneburg, M. Nagel, and G. Brunner, Z. Phys. A **291**, 113 (1979).

Journal of the Physical Society of Japan
Vol. 78, No. 3, March, 2009, 035003

Production and Decay Properties of ^{263}Hs

Daiya KAJI*, Kouji MORIMOTO, Nozomi SATO[1], Takatoshi ICHIKAWA, Eiji IDEGUCHI[2], Kazutaka OZEKI, Hiromitsu HABA, Hiroyuki KOURA[3], Yuki KUDOU, Akira OZAWA[4], Takayuki SUMITA[5], Takayuki YAMAGUCHI[6], Akira YONEDA, Atsushi YOSHIDA, and Kosuke MORITA

RIKEN Nishina Center, RIKEN, 2-1 Hirosawa, Wako, Saitama 351-0198
[1]*Department of Physics, Tohoku University, Sendai 980-8578*
[2]*Center for Nuclear Study, University of Tokyo, Wako, Saitama 351-0198*
[3]*Advanced Science Research Center, Japan Atomic Energy Agency, Tokai, Ibaraki 319-1195*
[4]*University of Tsukuba, Tsukuba, Ibaraki 305-8571*
[5]*Faculty of Science and Technology, Tokyo University of Science, Noda, Chiba 278-8510*
[6]*Department of Physics, Saitama University, Saitama 338-8570*

(Received November 15, 2008; accepted January 22, 2009; published March 10, 2009)

KEYWORDS: ^{263}Hs, gas-filled recoil ion separator, new isotope, hassium
DOI: 10.1143/JPSJ.78.035003

Since the first hassium ($Z = 108$) isotope of ^{265}Hs, which was produced via the cold fusion reaction of ^{208}Pb(^{58}Fe,n)^{265}Hs, was discovered by Münzenberg *et al.*,[1] six hassium isotopes of ^{264,266,267,269,270,271}Hs have been produced and their decay properties have been investigated in detail.[2–7] The α-decay of ^{263}Hs produced in the ^{209}Bi(^{55}Mn,n) reaction was first suggested by Oganessian *et al.*,[8] although no information about the decay property of ^{263}Hs, such as α-decay energy, was reported. Additionally, the possible production of ^{267}Ds ($Z = 110$) by using the ^{209}Bi(^{59}Co,n)^{267}Ds reaction was also reported by Ghiorso *et al.*[9] The discussion was based on the α-decay daughter of ^{263}Hs and the followed decay chains, although no decay of ^{263}Hs was detected in the study. In this work, our aim was to produce ^{263}Hs directly and to determine its decay properties for the first time.

The experiment was performed at the linear accelerator (RILAC) facility in RIKEN (The Institute of Physical and Chemical Research) from June 19 to 25, 2008. The isotope of ^{263}Hs was produced by two different reactions of ^{206}Pb(^{58}Fe,n) and ^{208}Pb(^{56}Fe,n). The projectiles of ^{58}Fe and ^{56}Fe with the charge state 13+ were extracted from the 18-GHz ECR ion source and accelerated by using the RILAC. The beams of ^{58}Fe with 287.7 MeV and ^{56}Fe with 280.4 MeV were extracted from the RILAC. The absolute accuracy of the beam energy measurement was $\pm$0.3 MeV. The typical beam intensities on the target were 4.5×10^{12} s^{-1} (corresponding to 0.75 pμA) for ^{58}Fe and 2.3×10^{12} s^{-1} (corresponding to 0.38 pμA) for ^{56}Fe.

The target was prepared by vacuum evaporation of metallic ^{206}Pb and ^{208}Pb on a 30 μg/cm^2 carbon backing foil. The target thicknesses were 400 μg/cm^2 for ^{206}Pb (Enrichment 99.3%) and 440 μg/cm^2 for ^{208}Pb (Enrichment 98.4%). A thin protection layer of approximately 10 μg/cm^2 of carbon covers the target surface in the downstream direction. The energy losses of the beam in the target were evaluated to be 3.9 MeV for ^{58}Fe in ^{206}Pb and 4.3 MeV for ^{56}Fe in ^{208}Pb using a stopping power table.[10] The beam energy at the middle of the target was estimated to be 285.0 MeV for ^{58}Fe and 277.5 MeV for ^{56}Fe, which correspond to the excitation energies of 16.2 and 16.0 MeV, respectively, when we use the mass table of Audi and Wapstra[11] for the projectile and target masses and that of Myers and Swiatecki[12] for the compound nucleus. Sixteen targets were mounted on a ϕ30 cm wheel, which rotated at 3000 rpm, to withstand the high intensity beam.

Reaction products were separated in flight from the beams by using a gas-filled recoil ion separator, GARIS, and were guided into a detector box installed at a focal plane of the GARIS. The separator was filled with a helium gas at a pressure of 86 Pa. A magnetic rigidity $B\rho$ was set to 2.05 Tm for ^{263}Hs measurement.

An evaporation residue (ER) and its successive radioactive decays were measured by using a system of TOF detectors and an array of a silicon position-sensitive detector (PSD) array installed at the focal plane of the GARIS. An identification of the products was based on genetic correlations of the mother and daughter nuclei. The energy resolution for decay α-particles measured only by the PSD was 45 keV in FWHM. However, when some energy was measured by the PSD and the remaining energy by one of the surrounding silicon detectors (SSDs), the energy resolution was 80 keV in FWHM. The singles counting rate of the PSD at the typical beam intensity was approximately 5 cps. The main components of the signals were due to the target recoils and scattered beam particles. The counting rate of the decay signals (anti-coincidence with timing counters) was approximately 0.3 cps. The detection system was monitored and calibrated by the α source of ^{241}Am and the ERs from the ^{nat}Ce + ^{58}Fe reaction.

During the 25-h irradiation of ^{206}Pb with the ^{58}Fe beam and 46-h irradiation of ^{208}Pb with the ^{56}Fe beam, 8 decay chains and 1 decay chain, respectively, have been observed. No spontaneous fission (SF) was detected in the measurements followed directly after the ER implantation in the PSD. The observed correlated decay chains are summarized in Table I: in this table, the measured decay energies, the time intervals between events, and the positions of decay events as well as that of the implantation events are indicated. The properties of decay events obtained by the irradiation of ^{58}Fe on ^{206}Pb coincide well with those by the irradiation of ^{56}Fe on ^{208}Pb. All decay chains were assigned to subsequent decays from ^{263}Hs. The decay data obtained in this work are summarized in Table II. As shown in the table, the decay properties of α2 or SF, α3 or SF, and α4 are in agreement with those of ^{259}Sg, ^{255}Rf, and ^{251}No.[13–15] The α3-decay energy of 8.44 MeV with the decay time of 6.195 s (chain 9) was observed in the present ^{208}Pb(^{56}Fe,n) reaction as one decay event, although no α-decay energy of 8.44 MeV was observed according to the reference data.[14] The ^{255}Rf has a small probability of EC decay branching according to the reference data.[14] There is a possibility that this α3-decay comes from the EC decay product ^{255}Lr, which has decay energies of 8.41 and 8.36 MeV with the half-life of 22 s.[15] Three groups of α-decay energies for ^{263}Hs are observed. The mean α-decay energies of the three groups are 10.82,

*E-mail: daiya@riken.jp